Fixed equilibria of point vortices in symmetric multiply connected domains

Takashi Sakajo
Department of mathematics, Hokkaido University
PRESTO, Japan Science and Technology Agency

PACS:47.10A-, 45.15.ki

Abstract

The paper provides with symmetric fixed configurations of point vortices in multiply connected domains in the unit circle with many circular obstacles. When the circular domain is invariant with respect to the rotation around the origin by the degree of $2\pi/M$, a regular M-polygonal ring configuration of identical point vortices becomes a fixed equilibrium. On the other hand, when we assume a special symmetry, called the folding symmetry, on the circular domain, we find a fixed equilibrium in which M point vortices with the positive unit strength and M point vortices with the negative unit strength are arranged alternately at the vertices of a $2M$-polygon. We also investigate the stability of these fixed equilibria and their bifurcation for a special circular domain with the rotational symmetry as well as the folding symmetry. Furthermore, we discuss fixed equilibria in non-circular multiply connected domains with the same symmetries. We give sufficient conditions for the conformal mappings, by which fixed equilibria in the circular domains are mapped to those in the general multiply connected domains. Some examples of such conformal mappings are also provided.

1 Introduction

Let us consider incompressible and inviscid flows in two-dimensional multiply connected domains that contain many solid obstacles. This kind of flow arises in many fluid problems associated with geophysical flows in coastal regions, inland lakes and rivers, since they usually contain many islands in their flow domains. In material sciences, one can represent a flow domain in porous media by a multiply connected one. Moreover, when the obstacles are allowed to move according to the flow, they are regarded as a simple mathematical model for swimming fish and falling leaves. Thus mathematical study of the flows in multiply connected domains contributes to the understanding of fundamental interactions between the solid-bodies and the flows. However, in spite of its importance, its mathematical theory is far from being complete.

In some applications, it is important to consider stationary configurations of vortex structures in multiply connected domains with certain symmetries. For example, the flow domain of a thin circular mixing container with multiple mixing devices as in Figure 1(a) becomes a multiply connected domain. When these mixing devices are fixed in the container according to the symmetry with respect to rotation, the domain acquires a rotational symmetry. Then stationary vortex structures may prevent an efficient mixing in the device, since fluid particles hardly move into the neighborhood of the vortices. Another interesting symmetric multiply connected domain arises, when one considers a design of an airfoil wing. Figure 1(b) is a triply connected exterior domain, in which two inclined plates are attached to a main plate. This is a two-dimensional model for

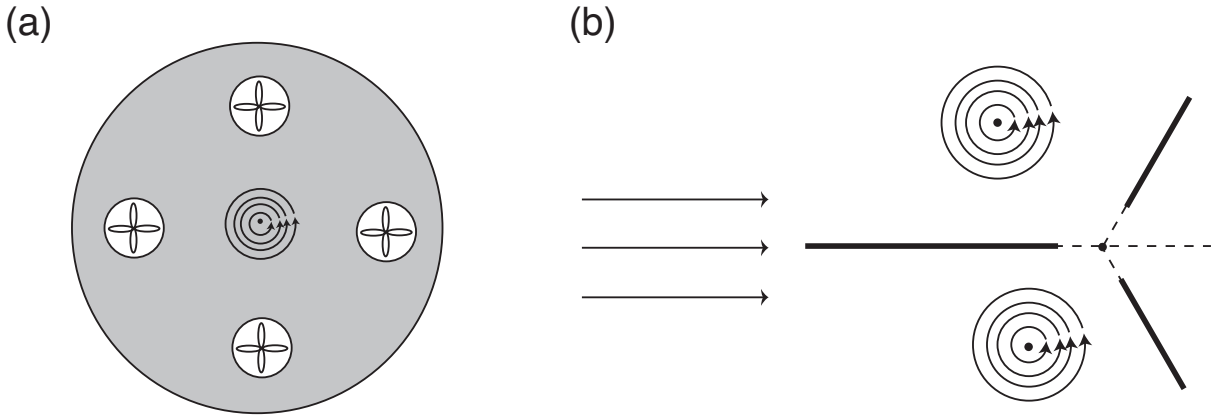

Figure 1: (a) A model of a mixing device that has four mixing rods, which defines a multiply connected domain with a rotational symmetry. If there exists a stationary vortex structure, an efficient mixing is prevented due to the existence of the vortex. (b) A two-dimensional model of "Kasper wing". The lift on the wing can be enhanced by trapping vortex structures between three plates. The flow domain is a triply connected exterior domain with three plates that is symmetric with respect to the horizontal line.

a wing designed by Kasper, which is known as "Kasper wing". He suggested that stationary vortex structures trapped between the plates can enhance the lift on the wing in the presence of a uniform flow. This concept has been examined by many researches. For instance, Saffman and Sheffield[17] investigated a free point vortex over a single plate, in which they found many fixed equilibria that enhance the lift. The flow domain in Figure 1(b) is symmetric with respect to the horizontal line, which gives rise to a problem of finding fixed equilibria in the symmetric multiply connected domain.

There is a connection between fixed point equilibria and a statistical dynamics of point vortices. The most probable statistic sate of a neutral point-vortex *gas* system in a two-dimensional domain Ω is described by solutions of $-\Delta\psi = \rho \sinh \psi$ in Ω with the boundary condition $\nabla\psi \cdot \boldsymbol{n} = 0$ on $\partial\Omega$, in which ρ is a certain parameter[16]. Bartolucci[2] proves that the solution of the sinh-Poisson equation converges to a stationary stable configuration of point vortices as $\rho \to 0$. Therefore, finding fixed equilibria of point vortices in multiply connected domains helps us understand the statistical properties of many point-vortex system in the multiply connected domains.

Recently, Crowdy and Marshall[4] gave an analytic formula for the complex potential function in a multiply connected domain inside the unit circle with many circular obstacles, which is called the *circular domain*. The circular domain is regarded as a canonical multiply connected domain, since it is mathematically shown that for every multiply connected domain with many holes, there exists a conformal mapping that maps the domain to a circular domain with the same number of circular obstacles[15]. Thanks to the analytic formula, an analytic representation of the uniform flows past circular obstacles is derived[7], and we can compute some important quantities such as the forces on the obstacles[8] and the flux between them[4]. Moreover, the analytic formula makes us possible to deal with the dynamics of point vortices, in which the vorticity concentrates point-wise like Dirac's δ functions. The point vortex evolves as if it were a material point, since its strength, which is equivalent to the circulation around the point, is conserved according to Kelvin's circulation theorem. Thus the motion of the N point vortices is regarded as one of the simplest mathematical descriptions of the vortex interactions.

Let $\{\zeta_\lambda(t) \in \mathbb{C} | \lambda = 0, \ldots, M-1\}$ denote the positions of the point vortices and $\{\Gamma_\lambda \in \mathbb{R} | \lambda = 0, \ldots, M-1\}$ be their strengths. Then the equation of motion is described by a Hamiltonian dynamical system with N degrees of freedom in the following complex form[12, 16]:

$$\Gamma_\lambda \frac{d\zeta_\lambda}{dt} = -2\mathrm{i}\frac{\partial H}{\partial \zeta_\lambda^*}, \qquad \lambda = 0, \ldots, N-1, \tag{1}$$

which is referred to as the *N-vortex problem*. The Hamiltonian $H = H(\zeta_0, \zeta_0^*, \cdots, \zeta_{N-1}, \zeta_{N-1}^*)$ is conventionally called the *Kirchhoff-Routh path function*, and z^* symbolizes the complex conjugation of z. The analytic formula for the Kirchhoff-Routh path function for the circular domains was provided by Crowdy and Marshall[4], with which the explicit representation of the equation (1) has been derived by Sakajo[18].

In the present paper, we are concerned with stationary configurations of the N point vortices in the circular domains. Since such fixed configurations are basic flows that describe interactions between solid-bodies and the flow surrounding them, they contribute to many fluid problems in multiply connected domains as a catalogue of vortex patterns like the one for the simply connected domain in Campbell and Ziff [3]. Now, let us remember that we have two kinds of stationary configurations of the point vortices. When the N point vortices never move throughout their evolution, the configuration of the point vortices is called a *fixed equilibrium*, which satisfies the following algebraic equations:

$$\frac{\partial H}{\partial \zeta_\lambda^*} = 0, \qquad \lambda = 0, \ldots, N-1. \tag{2}$$

On the other hand, when the N point vortices evolve without changing their relative distances, the configuration is called a *relative equilibrium*, which is obtained by solving the following equations for the relative distances between the point vortices, $l_{\alpha\lambda}^2 = |\zeta_\lambda - \zeta_\alpha|^2$:

$$\frac{d}{dt} l_{\alpha\lambda}^2 = 0, \qquad 0 \le \alpha < \lambda \le N-1. \tag{3}$$

Many results and references on fixed and relative equilibria in the unbounded plane and on the sphere are available in the book of Newton[16]. In this paper, assuming a certain symmetry in the configuration of point vortices, we reduce the algebraic equations (2) and (3) to simpler ones. Then we solve the reduced equations for given strengths of the point vortices. The approach brings us many symmetric stationary configurations of the point vortices as we see in [11, 13, 14].

This paper consists of six sections. In the next section, we give a summary of the mathematical formulation for the N-vortex problem in the circular domains given in [4, 18]. In § 3, we consider the circular domain that is symmetric with respect to the rotation around the origin by the degree $2\pi/M$. Then we obtain fixed configurations of M point vortices with the same strength. In § 4, introducing a special symmetry, called the *folding symmetry*, to the circular domain, we obtain fixed configurations of point vortices with the positive and the negative unit strengths. As an application of the results in §§ 3 and 4, we investigate the stability of the fixed equilibria and their bifurcation for a special circular domain that has the rotational symmetry as well as the folding symmetry. In addition, in § 5, we discuss fixed equilibria in general, non circular, multiply connected domains with the same symmetries. Generally, fixed equilibria in the circular domain are not necessarily mapped to those in the domain by the conformal mapping. However, we can give sufficient conditions that make fixed equilibria invariant with respect to the conformal mapping together with some examples. The last section is the conclusion and discussion.

2 Equation of motion for N point vortices in circular domains

Let us specify the geometry of multiply connected domains to describe the equation of motion for the N point vortices. The circular domain $\mathcal{D}_\zeta$ is a bounded region inside the unit circle $|\zeta| < 1$ in the complex ζ-plane in which N circular obstacles $\{C_j | j = 0, \ldots, N-1\}$ are embedded. The centers and the radii of their circular boundaries are represented by $\delta_j \in \mathbb{C}$ and $q_j \in \mathbb{R}$ respectively. The conjugation map $\phi_j(\zeta)$ with respect to the unit circle associated with the circle C_j is given by

$$\phi_j(\zeta) = \delta_j^* + \frac{q_j^2}{\zeta - \delta_j}, \qquad j = 0, \ldots, N-1,$$

with which we define the Möbius map $\vartheta_j(\zeta)$ by

$$\vartheta_j(\zeta) \equiv \phi_j^*(\zeta^{-1}) = \delta_j + \frac{q_j^2 \zeta}{1 - \delta_j^* \zeta}.$$

Here we use the following notations for the conjugation of map $\phi(\zeta)$:

$$(\phi(\zeta))^* = \phi^*(\zeta^*), \qquad (\phi(\zeta^*))^* = \phi^*(\zeta).$$

The infinite free group of maps generated by $\vartheta_j(\zeta)$ and its inverse $\vartheta_j^{-1}(\zeta)$ is called the *Schottky group*, denoted by Θ. We also introduce a subset Θ'' of the Schottky group by removing the identity map and all inverse mappings from Θ, with which the Schottky-Klein prime function $\omega(\zeta, \alpha)$ is defined by

$$\omega(\zeta, \alpha) = (\zeta - \alpha)\omega'(\zeta, \alpha), \qquad \omega'(\zeta, \alpha) = \prod_{\theta_i \in \Theta''} \frac{(\theta_i(\zeta) - \alpha)(\theta_i(\alpha) - \zeta)}{(\theta_i(\zeta) - \zeta)(\theta_i(\alpha) - \alpha)}. \tag{4}$$

Then, for given N point vortices $\{\zeta_\lambda \in \mathcal{D}_\zeta | \lambda = 0, \ldots, N-1\}$ and their strengths $\{\Gamma_\lambda \in \mathbb{R} | \lambda = 0, \ldots, N-1\}$, the Kirchhoff-Routh path function is represented by

$$H^{(\zeta)}(\zeta_0, \zeta_0^*, \ldots, \zeta_{N-1}, \zeta_{N-1}^*) = \sum_{\lambda=0}^{N-1} \sum_{\alpha=\lambda+1}^{N-1} \Gamma_\lambda \Gamma_\alpha G(\zeta_\lambda; \zeta_\alpha) - \frac{1}{2} \sum_{\lambda=0}^{N-1} \Gamma_\lambda^2 \mathcal{R}(\zeta_\lambda; \zeta_\lambda^*), \tag{5}$$

in which

$$G(\zeta; \alpha) = -\frac{1}{2\pi} \log \left| \frac{1}{\alpha} \frac{\omega(\zeta, \alpha)}{\omega(\zeta, \alpha^{*-1})} \right|,$$

and

$$\mathcal{R}(\alpha; \alpha^*) = \frac{1}{4\pi} \log \left| \frac{\omega'(\alpha, \alpha)\omega'^*(\alpha^{-1}, \alpha^{-1})}{\alpha^2 \omega(\alpha, \alpha^{*-1}) \omega^*(\alpha^{-1}, \alpha^*)} \right|.$$

The function $G(\zeta, \alpha)$ is the Green function satisfying the Poisson equation in $\mathcal{D}_\zeta$ with Dirichlet boundary condition. The function $\mathcal{R}$ is called the *Robin function*[10], See the paper [4] for the detailed derivation of the formula.

The equation of motion for the N point vortices in $\mathcal{D}_\zeta$ is derived from (1) with (5) as follows[18]:

$$\frac{d\zeta_\lambda}{dt} = \frac{\mathrm{i}}{2\pi} \sum_{\alpha \neq \lambda}^{N-1} \Gamma_\alpha \left(\frac{\omega_\zeta^*(\zeta_\lambda^*, \zeta_\alpha^*)}{\omega^*(\zeta_\lambda^*, \zeta_\alpha^*)} - \frac{\omega_\zeta^*(\zeta_\lambda^*, \zeta_\alpha^{-1})}{\omega^*(\zeta_\lambda^*, \zeta_\alpha^{-1})} \right) - \frac{\mathrm{i}}{2\pi} \Gamma_\lambda \frac{\omega_\zeta^*(\zeta_\lambda^*, \zeta_\lambda^{-1})}{\omega^*(\zeta_\lambda^*, \zeta_\lambda^{-1})}, \quad \lambda = 0, \ldots, N-1. \tag{6}$$

The two terms in the summation of the right hand side of (6) represent the contribution to the velocity field at ζ_λ from the point vortex ζ_α and its mirror image with respect to the unit circle

ζ_α^{*-1}. The last term gives the self-interaction between the point vortex ζ_λ and its mirror image ζ_λ^{*-1}. In the equation, the function $\omega_\zeta(\zeta,\alpha)/\omega(\zeta,\alpha)$ is represented by

$$\frac{\omega_\zeta(\zeta,\alpha)}{\omega(\zeta,\alpha)} = \frac{1}{\zeta-\alpha} + \sum_{\theta_j\in\Theta''}\left\{\frac{\theta_j'(\zeta)(\alpha-\zeta)}{(\theta_j(\zeta)-\alpha)(\theta_j(\zeta)-\zeta)} + \frac{\theta_j(\alpha)-\theta_j(\zeta)}{(\theta_j(\alpha)-\zeta)(\theta_j(\zeta)-\zeta)}\right\}, \tag{7}$$

in which $\theta_j'(\zeta) = \frac{d}{d\zeta}\theta_j(\zeta)$.

3 Fixed equilibria in circular domains with rotational symmetry

3.1 Problem settings

We consider fixed configurations of M point vortices with the same strength in the circular domains that are invariant with respect to the rotation around the origin by the degree $\theta_M = 2\pi/M$. The rotationally symmetric circular domain is constructed as follows. We set D circular obstacles in the unit circle, whose centers are located at $\delta_0^{(d)}$ and radii are $q_0^{(d)}$ for $d = 0,\ldots,D-1$. Then, rotating these obstacles by the degree $\lambda\theta_M$ for $\lambda = 1,\ldots,M-1$, we put new obstacles $C_\lambda^{(d)}$ of the same radius. Then, the center of $C_\lambda^{(d)}$ is located at $\delta_\lambda^{(d)} = s^\lambda\delta_0^{(d)}$ and its radius is $q_\lambda^{(d)} = q_0^{(d)}$, in which $s = \exp(\mathrm{i}\theta_M)$. Consequently, the circular domain contains the $M\times D$ obstacles. Note that the positions of the obstacles must be chosen so that they are disjoint with each other. In the similar manner, we are able to consider the rotationally symmetric circular domain inside the annulus, since the annulus is invariant with respect to the rotation around the origin. Examples of the rotationally symmetric circular domains for $M = 3$ are given in Figure 2.

Let $\{\zeta_\lambda(t)|\lambda = 0,\ldots,M-1\}$ denote the positions of the point vortices at time t, and their strengths are assumed to be $\Gamma_\lambda = 1$ without loss of generality. We now prove that if $\zeta_\lambda(0) = s^\lambda\zeta_0(0)$ at the initial moment, then $\zeta_\lambda(t) = s^\lambda\zeta_0(t)$ for $t\geq 0$. The proof proceeds in the following two steps. We first show the invariance of the M-vortex problem (6) for a special rotationally symmetric circular domain with M obstacles, say $\mathcal{D}_s$, whose centers are equally spaced along a circle of radius $a<1$. The center and the radius of the obstacle C_j in $\mathcal{D}_s$ is given by $\delta_j = as^j$ and $q_j = r$ for $j = 0,\ldots,M-1$ respectively. For a given a, the radius r can change until their circular boundaries are tangent to each other or the boundary of the unit circle, namely,

$$0 < r < \min(a\sin\theta_M, 1-a). \tag{8}$$

The generating function $\vartheta_j(\zeta)$ and its inverse $\vartheta_j^{-1}(\zeta)$ associated with the obstacle C_j are represented by

$$\vartheta_j(\zeta) = \frac{as^j + (r^2-a^2)\zeta}{1-as^{-j}\zeta}, \qquad \vartheta_j^{-1}(\zeta) = \frac{-as^j+\zeta}{r^2-a^2+as^{-j}\zeta}. \tag{9}$$

Then we extend the proof to the case of general circular domains that are invariant with respect to the rotation by the degree $2\pi/M$.

3.2 An observation of the Schottky group

We clarify some properties of the subset Θ'' of the Schottky group to prove the invariance with respect to the rotation. Let us introduce a finite permutation group generated by a cyclic permutation σ on $X = \{0,\ldots,M-1\}$,

$$\sigma = \begin{pmatrix} 0 & 1 & \cdots & M-2 & M-1 \\ 1 & 2 & \cdots & M-1 & 0 \end{pmatrix}. \tag{10}$$

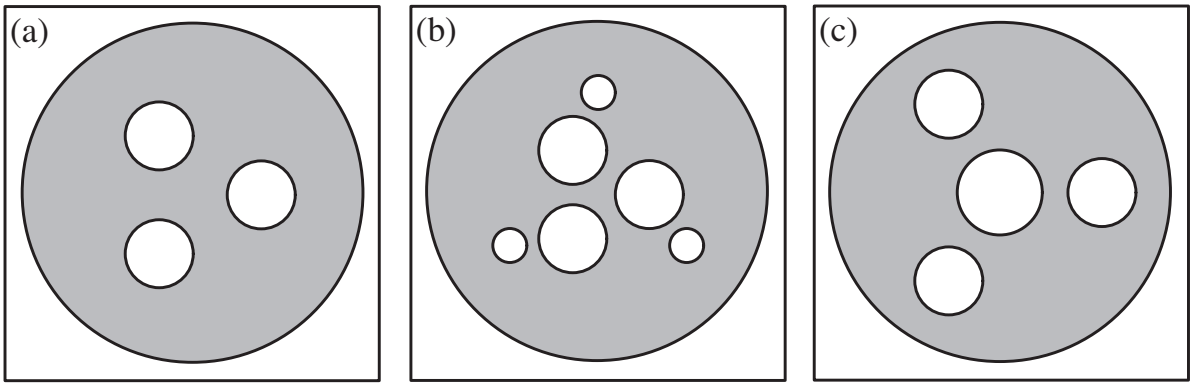

Figure 2: Examples of rotationally symmetric circular domains by the degree $2\pi/3$ for (a) $D = 1$ and (b) $D = 2$. (c) A rotationally symmetric circular domain in the annulus.

This group is given by $\Sigma = \{\sigma^0, \sigma^1, \sigma^2, \cdots, \sigma^{M-1}\}$, where σ^0 denotes the identity and $\sigma^{-k} = \sigma^{M-k}$. Let us note that σ^k defines a bijection on X, and $\sigma^k(j) = j + k \mod M$ for $j \in X$. Each element $\sigma^k \in \Sigma$ induces a permutation of the label of the generating functions by $\vartheta_j^{\pm 1} \mapsto \vartheta_{\sigma^k(j)}^{\pm 1}$. Since σ^k is bijective, the set of the generating functions is invariant under the action of σ^k, i.e., we have the identity $\left\{\vartheta_j^{\pm 1}\right\} \equiv \left\{\vartheta_{\sigma^k(j)}^{\pm 1}\right\}$ as a set.

In order to define the permutation of the label for all elements in the Schottky group Θ, we introduce a useful notion of *level* in all possible compositions of the generating functions as in [4]. The level-zero map is the identity map. The level-one map consists of the generating functions $\vartheta_j^{\pm 1}$ for $j = 0, \ldots, M-1$. The set containing all compositions of any two of the level-one maps that cannot be reduced to the identity map is called the level-two map. The higher level maps are similarly defined in a recursive manner. Then the permutation of the label for the level-l maps ($l \geq 2$) is defined by the l-product of the group Σ on X^l. Suppose that a level-l map $\theta_{\boldsymbol{j}}$ is expressed by the following lth composition of the generating functions,

$$\theta_{\boldsymbol{j}} = \vartheta_{j(1)} \circ \vartheta_{j(2)} \circ \cdots \circ \vartheta_{j(l)},$$

where each element $\vartheta_{j(i)}$ is either ϑ_j or ϑ_j^{-1} for $j = 0, \ldots, M-1$, and the map cannot be reduced to a lower level map. The l sequence of the labels $\boldsymbol{j} = (j(1), j(2), \cdots, j(l))$ is referred to as the *word* of the level-l map hereafter. The permutation $\boldsymbol{\sigma}_l^k(\boldsymbol{j}) \in \Sigma \times \cdots \times \Sigma \equiv \Sigma^l$ for $\boldsymbol{j} = (j(1), j(2), \cdots, j(l)) \in X^l$ is defined by

$$\boldsymbol{\sigma}_l^k(\boldsymbol{j}) = \left(\sigma_{j(1)}^k, \sigma_{j(2)}^k, \cdots, \sigma_{j(l)}^k\right),$$

which induces the permutation for the word of the level-l map $\theta_{\boldsymbol{j}}$ by

$$\theta_{\boldsymbol{\sigma}_l^k(\boldsymbol{j})} = \vartheta_{\sigma_{j(1)}^k} \circ \vartheta_{\sigma_{j(2)}^k} \circ \cdots \circ \vartheta_{\sigma_{j(l)}^k}.$$

The permutation of the word also defines a bijection on the level-l maps in the Schottky group. In other words, the set of the level-l maps $\{\theta_{\boldsymbol{j}}\} \subset \Theta$ is equivalent to the set $\left\{\theta_{\boldsymbol{\sigma}_l^k(\boldsymbol{j})}\right\}$. However, this claim is not trivial for the subset Θ'', since the identity and all the inverse maps are removed from the Schottky group. For example, suppose that a level-two map $\theta_{\boldsymbol{j}} = \vartheta_0 \vartheta_1^{-1}$ is in the subset

Θ'' for $M=2$, then its inverse $\vartheta_1\vartheta_0^{-1}$ is not contained in the subset. On the other hand, with a permutation of the word for the level-two maps,

$$\boldsymbol{\sigma}_2^1 = \begin{pmatrix} 0 & 1 \\ 1 & 0 \end{pmatrix} \times \begin{pmatrix} 0 & 1 \\ 1 & 0 \end{pmatrix},$$

we have $\theta_{\boldsymbol{\sigma}_2^1(\boldsymbol{j})} = \vartheta_1\vartheta_0^{-1} = \left(\vartheta_0\vartheta_1^{-1}\right)^{-1}$, which indicates that the permutation of the word $\boldsymbol{\sigma}_2^1$ does not define a map on the level-two maps in the subset Θ''. However, as a matter of fact, this is not the case. Let us remember that the Schottky-Klein prime function is uniquely defined from the subset Θ'' regardless of the choice of removing inverse maps[1]. This means that the subset Θ'' is characterized as follows. If we introduce an equivalence relation between elements θ_p and $\theta_q \in \Theta$ by

$$\theta_p \sim \theta_q \iff \theta_p = \theta_q^{-1},$$

then the subset Θ'' is regarded as the quotient set of Θ by $\sim$ minus the identity map e:

$$\Theta'' = (\Theta/\sim) \setminus \{e\}.$$

Hence, when we write $\theta \in \Theta''$, θ symbolizes a representing element in the equivalence class of θ in the Schottky group Θ. In this sense, in the example above, we can say that the map $\boldsymbol{\sigma}_2^1$ defines the identity map for the equivalence class of $\vartheta_0\vartheta_1^{-1}$. With the similar observation, we can show the permutation of the symbol $\boldsymbol{\sigma}_l^k$ gives a bijective map on the equivalence class of the level-l maps in the subset Θ''. Thus we have the identity between the sets of the equivalence class of the level-l maps $\theta_{\boldsymbol{j}} \in \Theta''$,

$$\{\theta_{\boldsymbol{j}}\} \equiv \left\{\theta_{\boldsymbol{\sigma}_l^k(\boldsymbol{j})}\right\} \subset \Theta''. \tag{11}$$

Now let us define another group S generated by $s = \exp(\mathrm{i}\theta_M)$. It is represented by $G = \{s^0, s^1, \cdots, s^{M-1}\}$, where s^0 is the identity and $s^{-k} = s^{M-k}$. Then the generating functions of the Schottky group $\vartheta_j^{\pm 1}(\zeta)$ satisfy the following relation for arbitrary j and k.

$$s^k\vartheta_j^{\pm 1}(\zeta) = \vartheta_{\sigma^k(j)}^{\pm 1}(s^k\zeta), \qquad \forall\zeta \in \mathcal{D}_s, \tag{12}$$

since we have

$$s^k\vartheta_j(\zeta) = \frac{as^{j+k} + (r^2-a^2)s^k\zeta}{1-as^{-j}\zeta} = \frac{as^q + (r^2-a^2)(s^k\zeta)}{1-as^{-q}(s^k\zeta)} = \vartheta_{\sigma^k(j)}(s^k\zeta),$$

due to $s^q = s^{j+k}$ for $q \equiv \sigma^k(j)$. For every level-l map $\theta_{\boldsymbol{j}} \in \Theta$, we obtain the similar relation,

$$s^k\theta_{\boldsymbol{j}}(\zeta) = \theta_{\boldsymbol{\sigma}_l^k(\boldsymbol{j})}(s^k\zeta), \tag{13}$$

since for the level-l map

$$\theta_{\boldsymbol{j}} = \vartheta_{j(1)} \circ \vartheta_{j(2)} \circ \cdots \circ \vartheta_{j(l)},$$

we have

$$\begin{aligned} s^k\theta_{\boldsymbol{j}}(\zeta) &= s^k\vartheta_{j(1)}(\vartheta_{j(2)} \circ \cdots \circ \vartheta_{j(l)}(\zeta)) \\ &= \vartheta_{\sigma^k(j(1))}(s^k(\vartheta_{j(2)} \circ \cdots \circ \vartheta_{j(l)}(\zeta))) \\ &\cdots \\ &= \vartheta_{\sigma^k(j(1))} \circ \vartheta_{\sigma^k(j(2))} \circ \cdots \circ \vartheta_{\sigma^k(j(l))}(s^k\zeta) \\ &= \theta_{\boldsymbol{\sigma}_l^k(\boldsymbol{j})}(s^k\zeta). \end{aligned}$$

Regarding the derivative of the level-l map $\theta_{\boldsymbol{j}} \in \Theta$, we obtain

$$\left(\frac{d}{d\zeta}\theta_{\boldsymbol{\sigma}_l^k(\boldsymbol{j})}\right)(s^k\zeta) = \left(\frac{d}{d\zeta}\theta_{\boldsymbol{j}}\right)(\zeta), \quad \forall\zeta \in \mathcal{D}_s. \tag{14}$$

For the generating function $\vartheta_j(\zeta)$, it is easy to see that

$$\frac{d}{d\zeta}\vartheta_{\sigma^k(j)}(s^k\zeta) = \frac{r^2}{(1-as^{-(j+k)}s^k\zeta)^2} = \frac{r^2}{(1-as^{-j}\zeta)^2} = \frac{d}{d\zeta}\vartheta_j(\zeta).$$

The same relation is obvious for the inverse of the generating function. For the level-l maps, we can show it by using the chain rule. For example, for a level-two map $\theta_{\boldsymbol{j}}(\zeta) = (\vartheta_p \circ \vartheta_q)(\zeta)$, we have

$$\frac{d}{d\zeta}\theta_{\boldsymbol{\sigma}_2^k(\boldsymbol{j})}(\zeta) \quad = \quad \frac{d}{dw}\vartheta_{\sigma^k(p)}(w) \times \frac{d}{d\zeta}\vartheta_{\sigma^k(q)}(\zeta), \tag{15}$$

where $w = \vartheta_{\sigma^k(q)}(\zeta)$. When we substitute $\zeta = s^k z$ to (15), it follows from (12) and (14) that we have

$$\begin{aligned}
\left(\frac{d}{d\zeta}\theta_{\boldsymbol{\sigma}_2^k(\boldsymbol{j})}\right)(s^k\zeta) &= \left(\frac{d}{dw}\vartheta_{\sigma^k(p)}\right)(\vartheta_{\sigma^k(q)}(s^k\zeta)) \times \left(\frac{d}{d\zeta}\vartheta_{\sigma^k(q)}\right)(s^k\zeta) \\
&= \left(\frac{d}{dw}\vartheta_{\sigma^k(p)}\right)(s^k\vartheta_q(\zeta)) \times \left(\frac{d}{d\zeta}\vartheta_{\sigma^k(q)}\right)(s^k\zeta) \\
&= \left(\frac{d}{dw}\vartheta_p\right)(\vartheta_q(\zeta)) \times \left(\frac{d}{d\zeta}\vartheta_q\right)(\zeta) = \left(\frac{d}{d\zeta}\theta_{\boldsymbol{j}}\right)(\zeta).
\end{aligned}$$

Since the relations (11), (13) and (14) have been proved for arbitrary level-l maps, we can omit the level subscript l in the permutation of the word. Hence, when we define the set of the permutations for the word of arbitrary elements $\theta_{\boldsymbol{j}} \in \Theta''$ by

$$\{\boldsymbol{\sigma}^k(\boldsymbol{j})\} = \bigcup_{l=1}^{\infty}\{\boldsymbol{\sigma}_l^k(\boldsymbol{j})\},$$

the results of this subsection are summarized as follows.

Lemma 3.1 *For the permutation $\boldsymbol{\sigma}^k(\boldsymbol{j})$ for the word of the element $\theta_{\boldsymbol{j}} \in \Theta$,*

(1) the map induces a bijection on Θ'' for all k, i.e., $\{\theta_{\boldsymbol{j}}\} = \left\{\theta_{\boldsymbol{\sigma}^k(\boldsymbol{j})}\right\} = \Theta''$,

(2) $s^k\theta_{\boldsymbol{j}}(\zeta) = \theta_{\boldsymbol{\sigma}^k(\boldsymbol{j})}(s^k\zeta), \qquad \forall\theta_{\boldsymbol{j}} \in \Theta, \quad \forall\zeta \in \mathcal{D}_s,$

(3) $\left(\frac{d}{d\zeta}\theta_{\boldsymbol{\sigma}^k(\boldsymbol{j})}\right)(s^k\zeta) = \left(\frac{d}{d\zeta}\theta_{\boldsymbol{j}}\right)(\zeta), \qquad \forall\theta_{\boldsymbol{j}} \in \Theta, \quad \forall\zeta \in \mathcal{D}_s.$

3.3 Invariance with respect to the rotation

Thanks to Lemma 3.1, it is now easy to show the following proposition.

Proposition 3.1 *Let $\{\zeta_\lambda(t)|\lambda = 0, \ldots, M-1\}$ denote the positions of the M point vortices with the unit strength at time t. Then, for the rotationally symmetric circular domain $\mathcal{D}_s$, if $\zeta_\lambda(0) = s^\lambda\zeta_0(0)$, we have $\zeta_\lambda(t) = s^\lambda\zeta_0(t)$ for $t \geq 0$, where $s = \exp(\mathrm{i}\theta_M)$.*

Proof: The proof is done by showing that $\dot{\zeta}_\lambda = s^\lambda \dot{\zeta}_0$ holds from (6) and (7). Let us set $\boldsymbol{q} = \boldsymbol{\sigma}^{-\lambda}(\boldsymbol{j})$. For the self-interaction term in the equation (6), it follows from the assumption $\zeta_\lambda = s^\lambda \zeta_0$ and Lemma 3.1 that we have

$$
\begin{aligned}
&\frac{\omega_\zeta(\zeta_\lambda, \zeta_\lambda^{*-1})}{\omega(\zeta_\lambda, \zeta_\lambda^{*-1})} = \frac{\omega_\zeta(s^\lambda\zeta_0, s^\lambda\zeta_0^{*-1})}{\omega(s^\lambda\zeta_0, s^\lambda\zeta_0^{*-1})} \\
&= \frac{1}{s^\lambda(\zeta_0 - \zeta_0^{*-1})} + \sum_{\theta_{\boldsymbol{j}} \in \Theta''} \left\{ \frac{\theta'_{\boldsymbol{j}}(s^\lambda\zeta_0)(s^\lambda\zeta_0^{*-1} - s^\lambda\zeta_0)}{(\theta_{\boldsymbol{j}}(s^\lambda\zeta_0) - s^\lambda\zeta_0^{*-1})(\theta_{\boldsymbol{j}}(s^\lambda\zeta_0) - s^\lambda\zeta_0)} + \frac{\theta_{\boldsymbol{j}}(s^\lambda\zeta_0^{*-1}) - \theta_{\boldsymbol{j}}(s^\lambda\zeta_0)}{(\theta_{\boldsymbol{j}}(s^\lambda\zeta_0^{*-1}) - s^\lambda\zeta_0)(\theta_{\boldsymbol{j}}(s^\lambda\zeta_0) - s^\lambda\zeta_0)} \right\} \\
&= s^{-\lambda}\frac{1}{(\zeta_0 - \zeta_0^{*-1})} + \sum_{\theta_{\boldsymbol{j}} \in \Theta''} \left\{ s^{-\lambda}\frac{\theta'_{\boldsymbol{q}}(\zeta_0)(\zeta_0^{*-1} - \zeta_0)}{(\theta_{\boldsymbol{q}}(\zeta_0) - \zeta_0^{*-1})(\theta_{\boldsymbol{q}}(\zeta_0) - \zeta_0)} + s^{-\lambda}\frac{\theta_{\boldsymbol{q}}(\zeta_0^{*-1}) - \theta_{\boldsymbol{q}}(\zeta_0)}{(\theta_{\boldsymbol{q}}(\zeta_0^{*-1}) - \zeta_0)(\theta_{\boldsymbol{q}}(\zeta_0) - \zeta_0)} \right\} \\
&= s^{-\lambda}\frac{1}{(\zeta_0 - \zeta_0^{*-1})} + \sum_{\theta_{\boldsymbol{q}} \in \Theta''} \left\{ s^{-\lambda}\frac{\theta'_{\boldsymbol{q}}(\zeta_0)(\zeta_0^{*-1} - \zeta_0)}{(\theta_{\boldsymbol{q}}(\zeta_0) - \zeta_0^{*-1})(\theta_{\boldsymbol{q}}(\zeta_0) - \zeta_0)} + s^{-\lambda}\frac{\theta_{\boldsymbol{q}}(\zeta_0^{*-1}) - \theta_{\boldsymbol{q}}(\zeta_0)}{(\theta_{\boldsymbol{q}}(\zeta_0^{*-1}) - \zeta_0)(\theta_{\boldsymbol{q}}(\zeta_0) - \zeta_0)} \right\} \\
&= s^{-\lambda}\frac{\omega_\zeta(\zeta_0, \zeta_0^{*-1})}{\omega(\zeta_0, \zeta_0^{*-1})},
\end{aligned}
$$

in which we use the equivalence of the sets $\{\theta_{\boldsymbol{j}}\} = \{\theta_{\boldsymbol{q}}\}$. The first term in the vortex-vortex interaction part of (6) is reduced as follows.

$$
\begin{aligned}
&\sum_{\alpha \neq \lambda} \frac{\omega_\zeta(\zeta_\lambda, \zeta_\alpha)}{\omega(\zeta_\lambda, \zeta_\alpha)} = \sum_{\alpha \neq \lambda} \frac{\omega_\zeta(s^\lambda\zeta_0, s^\alpha\zeta_0)}{\omega(s^\lambda\zeta_0, s^\alpha\zeta_0)} \\
&= \sum_{\alpha \neq \lambda} \left(\frac{1}{s^\lambda\zeta_0 - s^\alpha\zeta_0} + \sum_{\theta_{\boldsymbol{j}} \in \Theta''} \left\{ \frac{\theta'_{\boldsymbol{j}}(s^\lambda\zeta_0)(s^\alpha\zeta_0 - s^\lambda\zeta_0)}{(\theta_{\boldsymbol{j}}(s^\lambda\zeta_0) - s^\alpha\zeta_0)(\theta_{\boldsymbol{j}}(s^\lambda\zeta_0) - s^\lambda\zeta_0)} + \frac{\theta_{\boldsymbol{j}}(s^\alpha\zeta_0) - \theta_{\boldsymbol{j}}(s^\lambda\zeta_0)}{(\theta_{\boldsymbol{j}}(s^\alpha\zeta_0) - s^\lambda\zeta_0)(\theta_{\boldsymbol{j}}(s^\lambda\zeta_0) - s^\lambda\zeta_0)} \right\} \right) \\
&= s^{-\lambda} \sum_{\alpha \neq \lambda} \left(\frac{1}{(1 - s^{\alpha-\lambda})\zeta_0} + \sum_{\theta_{\boldsymbol{q}} \in \Theta''} \left\{ \frac{\theta'_{\boldsymbol{q}}(\zeta_0)(s^{\alpha-\lambda} - 1)\zeta_0}{(\theta_{\boldsymbol{q}}(\zeta_0) - s^{\alpha-\lambda}\zeta_0)(\theta_{\boldsymbol{q}}(\zeta_0) - \zeta_0)} + \frac{\theta_{\boldsymbol{\sigma}^{-\alpha+\lambda}(\boldsymbol{q})}(\zeta_0) - \theta_{\boldsymbol{q}}(\zeta_0)}{(\theta_{\boldsymbol{\sigma}^{-\alpha+\lambda}(\boldsymbol{q})}(\zeta_0) - \zeta_0)(\theta_{\boldsymbol{q}}(\zeta_0) - \zeta_0)} \right\} \right) \\
&= s^{-\lambda} \sum_{\beta=1}^{M-1} \left(\frac{1}{(1 - s^\beta)\zeta_0} + \sum_{\theta_{\boldsymbol{q}} \in \Theta''} \left\{ \frac{\theta'_{\boldsymbol{q}}(\zeta_0)(s^\beta - 1)\zeta_0}{(\theta_{\boldsymbol{q}}(\zeta_0) - s^\beta\zeta_0)(\theta_{\boldsymbol{q}}(\zeta_0) - \zeta_0)} + \frac{\theta_{\boldsymbol{\sigma}^{-\beta}(\boldsymbol{q})}(\zeta_0) - \theta_{\boldsymbol{q}}(\zeta_0)}{(\theta_{\boldsymbol{\sigma}^{-\beta}(\boldsymbol{q})}(\zeta_0) - \zeta_0)(\theta_{\boldsymbol{q}}(\zeta_0) - \zeta_0)} \right\} \right) \\
&= s^{-\lambda} \sum_{\beta=1}^{M-1} \frac{\omega_\zeta(\zeta_0, s^\beta\zeta_0)}{\omega(\zeta_0, s^\beta\zeta_0)},
\end{aligned}
$$

in which we put $\beta = \alpha - \lambda$. We can handle the second term in the interaction part of (6) in the same way. Consequently, taking the complex conjugate, we obtain $\dot{\zeta}_\lambda = s^\lambda \dot{\zeta}_0$, which finishes the proof.

□

We extend the proof of Proposition 3.1 to the case of the general circular domain with the rotational symmetry.

Theorem 3.1 *Suppose that the multiply connected circular domain is invariant with respect to the rotation around the origin by the degree $\theta_M = 2\pi/M$. Let $\{\zeta_\lambda(t) | \lambda = 0, \ldots, M-1\}$ denote the positions of the M point vortices with the unit strength at time t in the circular domain. Then, if $\zeta_\lambda(0) = s^\lambda\zeta_0(0)$ holds, then we have $\zeta_\lambda(t) = s^\lambda\zeta_0(t)$ for $t \geq 0$, where $s = \exp(\mathrm{i}\theta_M)$.*

Proof: Let us introduce another group of the permutations for the word of the maps in the Schottky group associate with the rotationally symmetric circular domain for general D. Instead of (10), we use the finite permutation group generated by a permutation on $M \times D$ integers,

$$\sigma : \begin{pmatrix} 0 & \cdots & M-1 & M & \cdots & 2M-1 & \cdots & (D-1)M & \cdots & DM-1 \\ 1 & \cdots & 0 & M+1 & \cdots & M & \cdots & (D-1)M+1 & \cdots & (D-1)M \end{pmatrix}.$$

For the rotationally symmetric domain inside the annulus, since the center circle is regarded as the additional $(M \times D+1)$th circular obstacle inside the unit circle, we use the following permutation as a generating element:

$$\sigma : \begin{pmatrix} 0 & \cdots & M-1 & M & \cdots & 2M-1 & \cdots & (D-1)M & \cdots & DM-1 & DM \\ 1 & \cdots & 0 & M+1 & \cdots & M & \cdots & (D-1)M+1 & \cdots & (D-1)M & DM \end{pmatrix}.$$

Both of them induce a bijection on the set of the generating functions of the Schottky group. Thus we define the permutation of the word for the level-l maps by an element in the l-product of the permutation group, which also induces a bijection on the set Θ''. Since we are able to show Lemma 3.1 for these new bijective permutation groups in the same way, the proof of the theorem is finished by following the proof of Proposition 3.1.

□

3.4 Rotationally symmetric fixed equilibria

Theorem 3.1 claims that the rotationally symmetric configuration $\zeta_\lambda = s^\lambda \zeta_0$ remains unchanged for all time, if it holds at the initial moment. Hence, we reduce the system to a one-degree-of-freedom Hamiltonian dynamical system with the relation $\zeta_\lambda = s^\lambda \zeta_0$. Since the reduced system is integrable, the orbit of the M point vortices is simply observed by plotting the contour lines of the reduced Hamiltonian, which is given by

$$H_s^{(\zeta)}(\zeta_0) = \sum_{\lambda=0}^{M-1} \sum_{\alpha=\lambda+1}^{M-1} G(s^\lambda \zeta_0; s^\alpha \zeta_0) - \frac{1}{2} \sum_{\lambda=0}^{M-1} \mathcal{R}(s^\lambda \zeta_0; (s^\lambda \zeta_0)^*). \tag{16}$$

Figure 3 shows the contour plots of the Hamiltonian (16) for the sample circular domains given in Figure 2. Fixed equilibria of the identical three point vortices are represented by centers and saddles of the contour plots. Let us note that, because of the rotational symmetry, all fixed equilibria correspond to the configuration where the identical M point vortices are placed at the vertices of a regular M-polygon, which is called the *M-ring*. The M-rings at saddle points are unstable and those at centers are neutrally stable. The M-rings at the saddle points are connected by heteroclinic orbits. Each contour line except for the fixed equilibria and the heteroclinic orbits corresponds to a periodic orbit.

In what follows, we investigate fixed equilibria in the special circular domain $\mathcal{D}_s$ and discuss their bifurcation. Figure 4 shows the contour plots of Hamiltonian (16) in $\mathcal{D}_s$ for $M = 3$. The centers of the obstacles are equally spaced along the circle of radius $a = 0.5$ and we change the radius r of the obstacles. For all r, we always have an unstable 3-ring located at $\zeta_\lambda = R_a \exp(2\pi\lambda/3)$ with a certain $R_a > a + r$ near the obstacles. As the radius r increases, there emerge two other 3-rings located at $\zeta_\lambda = r \exp(\mathrm{i}(2\pi\lambda/3 + \pi/3))$ with some $r = R_b$ and $r = R_c$ ($R_b < R_c$) between the obstacles as we see in Figure 4(c). The one at R_b is unstable and the other one at R_c is neutrally stable. For the sake of reference, we identify the three M-rings as follows.

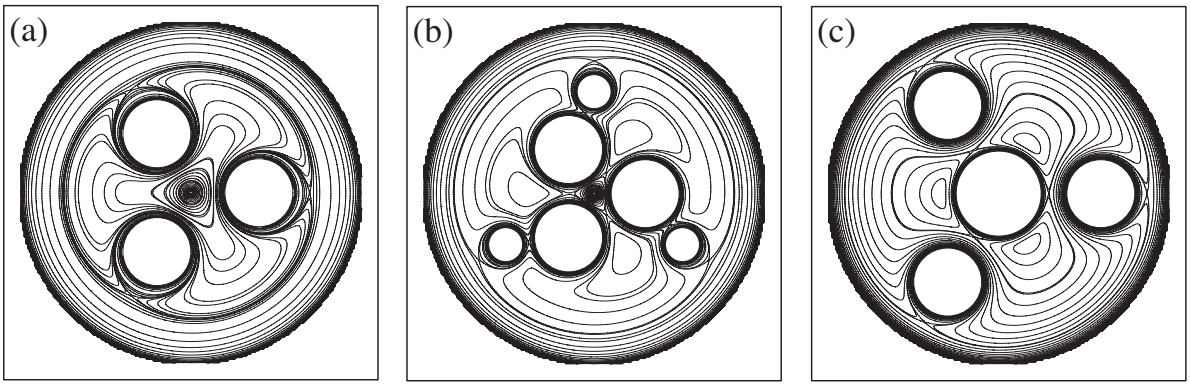

Figure 3: Contour plots of the Hamiltonian (16) for the rotationally symmetric circular domains corresponding to those in Figure 2. Fixed equilibria of three point vortices, which form equilateral triangles, are located at saddles or centers of the contour lines.

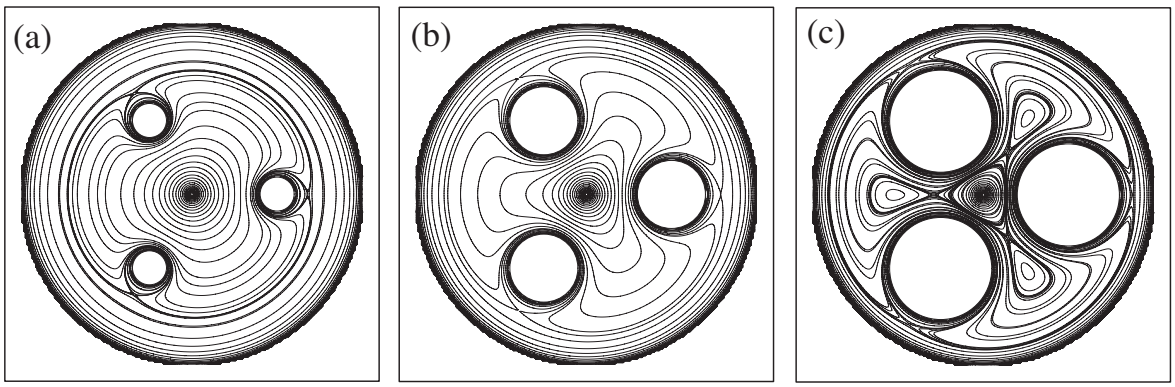

Figure 4: Contour plots of the Hamiltonian (16) in the circular domain $\mathcal{D}_s$ with three obstacles for (a) $a = 0.5$ and $r = 0.1$; (b) $a = 0.5$ and $r = 0.2$; (c) $a = 0.5$ and $r = 0.3$. While the centers of the circular obstacles are unchanged, their radii are changed. As r increases, the topological structure of the contour lines changes, at which a saddle fixed equilibrium between the circular obstacles is generated.

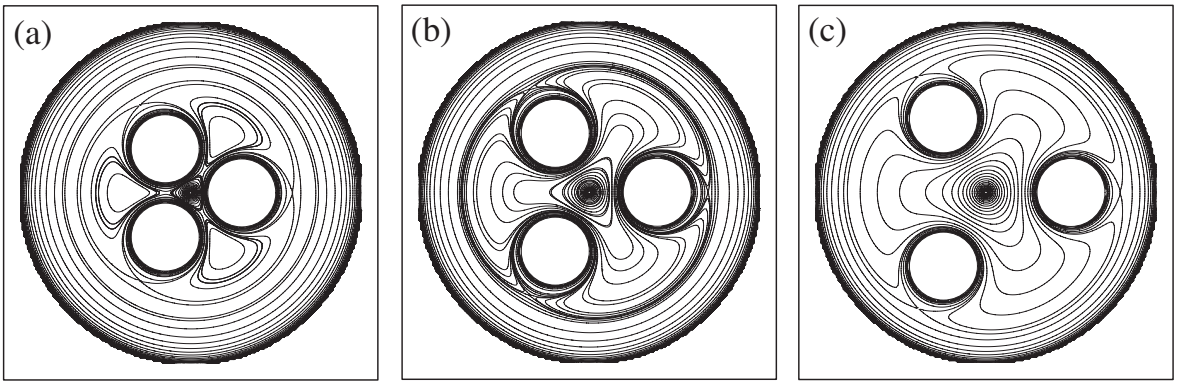

Figure 5: Contour plots of the Hamiltonian (16) in $\mathcal{D}_s$ with three obstacles for (a) $a = 0.3$ and $r = 0.2$; (b) $a = 0.4$ and $r = 0.2$; (c) $a = 0.5$ and $r = 0.2$. In this case, we change the center of the circular boundaries.

(1) $\zeta_M^{(a)}$: the unstable M-ring located at $R_a \exp(\mathrm{i}2\pi\lambda/M)$ with some $R_a > r + a$,

(2) $\zeta_M^{(b)}$: the unstable M-ring located at $R_b \exp(\mathrm{i}(2\pi\lambda/M + \pi/M))$,

(3) $\zeta_M^{(c)}$: the neutrally stable M-ring located at $R_c \exp(\mathrm{i}(2\pi\lambda/M + \pi/M))$ with $R_c < R_b$.

Figure 5 shows the contour plots of the Hamiltonian (16) for $M = 3$ when we fix r and change a. We observe the unstable 3-ring $\zeta_3^{(a)}$ in all panels of the figure. On the other hand, as the obstacles approach the origin, the unstable 3-ring $\zeta_3^{(b)}$ and the neutrally stable 3-ring $\zeta_3^{(c)}$ emerge as we see in Figure 5(a). From these observations, we expect that there always exists the unstable 3-ring $\zeta_3^{(a)}$, while the unstable 3-ring $\zeta_3^{(b)}$ and the neutrally stable 3-ring $\zeta_3^{(c)}$ appear when the distance between the obstacles exceeds some critical values of a and r. To describe this bifurcation quantitatively, we plot in Figure 6 the locations of the 3-rings, i.e., the values of R_a, R_b and R_c, versus the radius r for $a = 0.3$ and $a = 0.5$. As r approaches the maximum limit at which the obstacles are tangent to each other, the position of the unstable 3-ring $\zeta_3^{(b)}$ converges to the tangent point, namely $R_b \to a\cos(\pi/3)$, which are drawn as a horizontal line in each figure. Moreover, both of the figures also illustrate that a saddle-shaped bifurcation occurs at a certain critical value of the radius $r_c(a)$ that depends on a. The critical radius is plotted in Figure 7 for various a, which indicates a linear dependence of $r_c(a)$ on $a \ll 1$. On the other hand, the critical value deviates from the linear curve as a increases. This is because the boundary of the unit circle affects the positions of the 3-rings, $\zeta_3^{(b)}$ and $\zeta_3^{(c)}$.

The same bifurcation is observed for other M. Figure 8 shows the contour plots of the Hamiltonian (16) in $\mathcal{D}_s$ for $M = 4, 5, 6$. This indicates that the unstable M-ring $\zeta_M^{(a)}$ always exists, and the unstable M-ring $\zeta_M^{(b)}$ and the neutrally stable M-ring $\zeta_M^{(c)}$ appear, when the distances between the obstacles get closer. Since the fixed equilibria $\zeta_M^{(b)}$ and $\zeta_M^{(c)}$ emerge due to the same saddle-shaped bifurcation, we plot the critical radius $r_c(a)$ for $M = 4, 5, 6$ in Figure 9, which also shows the linear dependence of $r_c(a)$ on $a \ll 1$.

Let us finally discuss the existence of relative equilibria in $\mathcal{D}_s$. As we have already mentioned, each contour line of the Hamiltonian corresponds to a periodic orbit except for the fixed equilibria and the heteroclinic orbits. Among the periodic orbits, if we found a periodic orbit in which the relative distances between the point vortices are unchanged throughout the evolution, the periodic

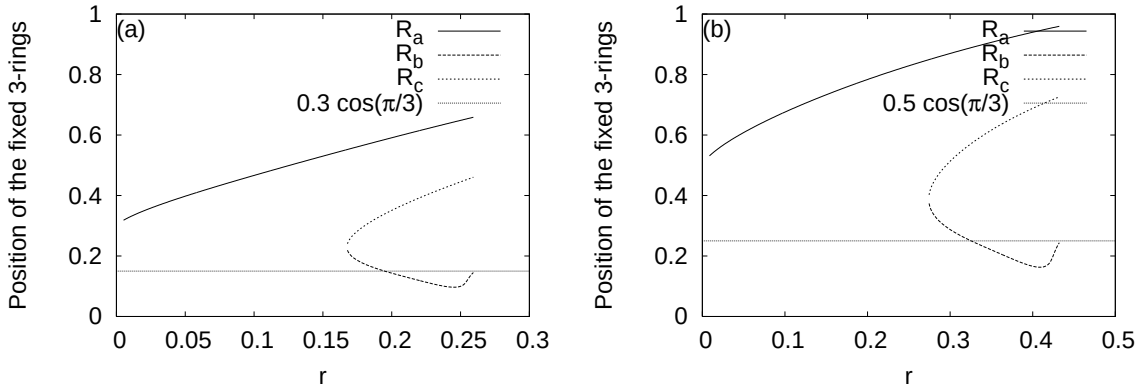

Figure 6: Plots of the radii R_a, R_b and R_c of the 3-rings $\zeta_3^{(a)}$, $\zeta_3^{(b)}$ and $\zeta_3^{(c)}$ as functions of the radius of the obstacles r for (a) $a = 0.3$ and (b) $a = 0.5$. As r increases, a saddle-shaped bifurcation occurs at a certain critical point.

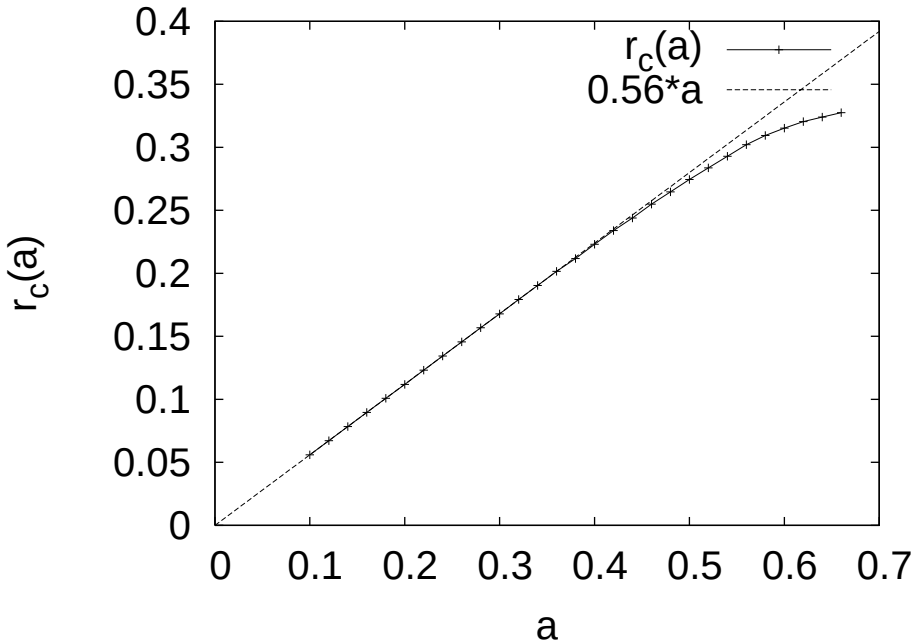

Figure 7: Plot of the critical radius $r_c(a)$ where the saddle-shaped bifurcation of the 3-rings occurs. The critical values are aligned along a line as $a \to 0$.

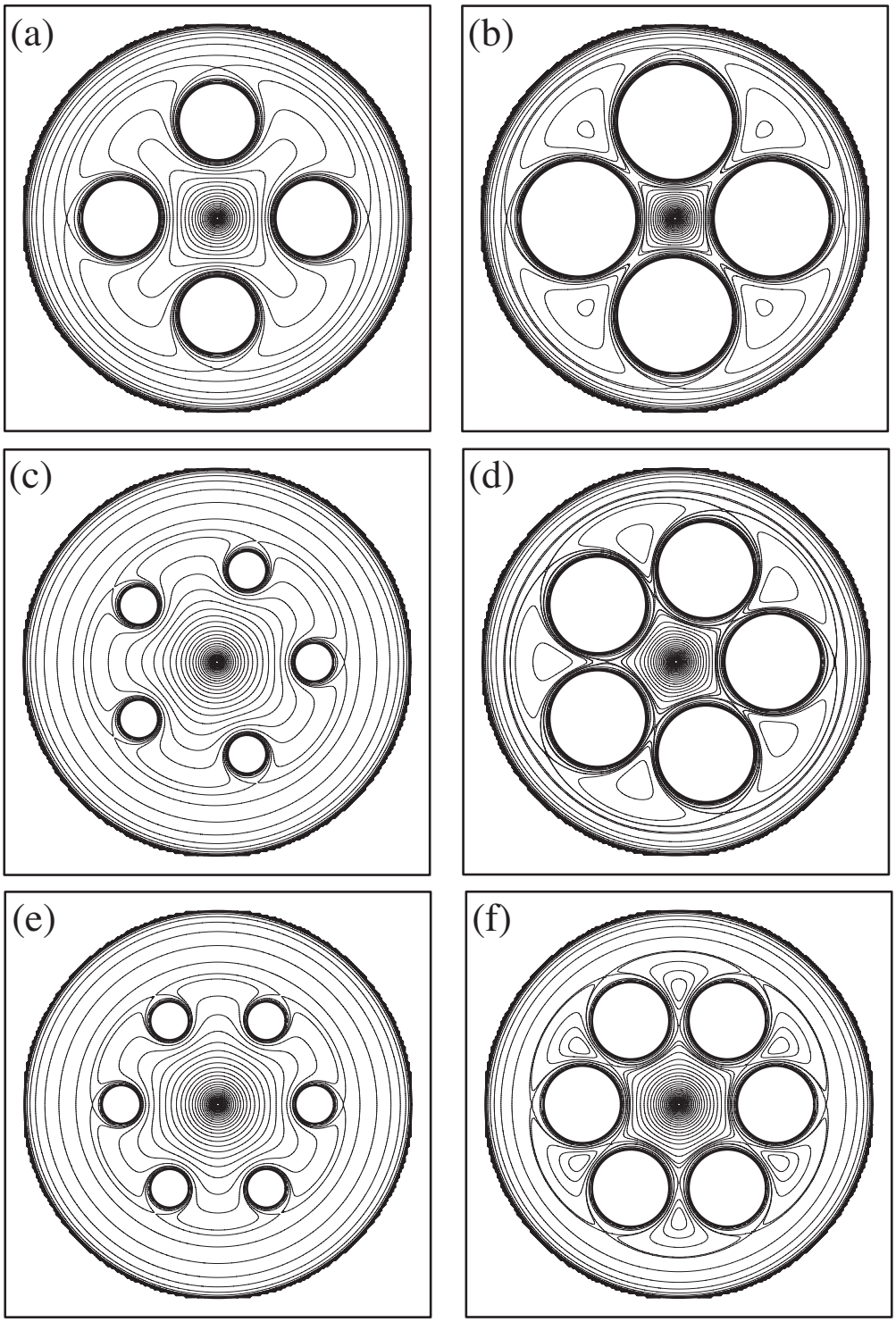

Figure 8: Contour plots of the Hamiltonian (16) in $\mathcal{D}_s$ for (a) $a = 0.5$, $r = 0.2$, $M = 4$ and (b) $a = 0.5$, $r = 0.3$, $M = 4$; (c) $a = 0.5$, $r = 0.1$, $M = 5$ and (d) $a = 0.5$, $r = 0.25$, $M = 5$; (e) $a = 0.5$, $r = 0.1$, $M = 6$ and (f) $a = 0.5$, $r = 0.2$, $M = 6$.

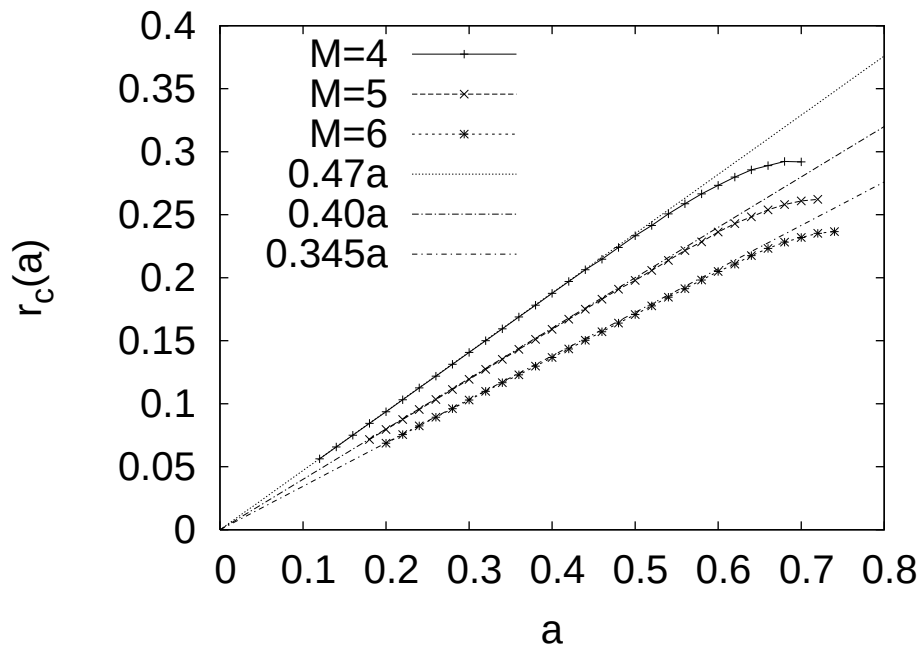

Figure 9: Plots of the critical values $r_c(a)$ where the saddle-shaped bifurcation of the M-rings occurs for $M = 4, 5, 6$. The critical values have the similar linear dependence on a as we observe in Figure 7 regardless of the number of the obstacles M.

orbit corresponds to a relative equilibria. For instance, when we see the contour lines in Figure 5, the periodic orbits in the neighborhood of the origin and the boundary of the unit circle could represent relative equilibria, since they look circles whose center are at the origin. This is checked numerically by observing the following difference between the maximum and the minimum values of the Hamiltonian,

$$\Delta_H(|\zeta|) \equiv \max_{0\le\theta<2\pi} H_s^{(\zeta)}\left(|\zeta|e^{\mathrm{i}\theta}\right) - \min_{0\le\theta<2\pi} H_s^{(\zeta)}\left(|\zeta|e^{\mathrm{i}\theta}\right), \qquad 0 < |\zeta| < 1.$$

If $\Delta_H = 0$ for some ζ, the contour line through the point ζ coincides with a circle, which means the corresponding orbit is a relative M-ring. Figure 10 shows the difference $\Delta_H(|\zeta|)$ for the contour plots given in Figure 5(a)-(c), which indicates that $\Delta_H \neq 0$ for all cases. Thus we find no relative equilibria in the rotationally symmetric circular domains.

4 Fixed equilibria in circular domains with folding symmetry

4.1 Problem settings

We consider another type of fixed equilibria of point vortices with the strengths of opposite signs in the circular domains with a special symmetry, which is explained by using a circular domain with eight obstacles in Figure 11. Dividing the circular domain into eight subregions, we assign the labels $\{D_\lambda | \lambda = 0, \ldots, 7\}$ to the subregions. The subdomains with the even labels are painted in gray color, and those with the odd labels are painted in white, in order to distinguish them. Note that the order of labeling of the subdomains seems to be unusual, but it is convenient to

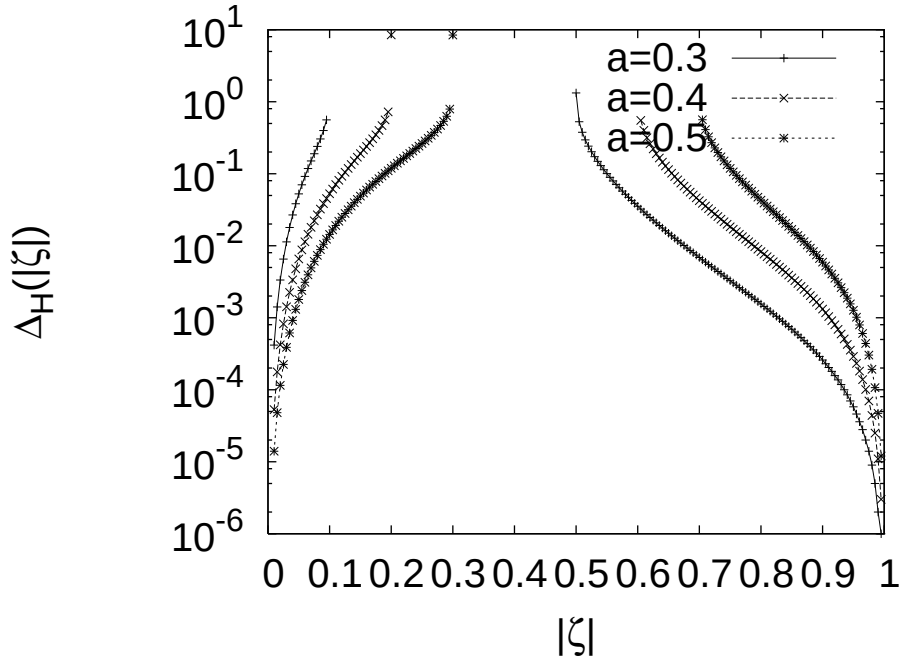

Figure 10: Plots of the difference $\Delta_H(|\zeta|)$ between the maximum and the minimum of the Hamiltonian (16) along the circle with radius $|\zeta|$ for $a = 0.3$, 0.4, 0.5. Since $\Delta_H(|\zeta|) \neq 0$, the orbits of the point vortices are not on circles, which indicates that no relative equilibrium exists.

describe the symmetry as follows. Let $\{\zeta_{2\lambda}, \zeta_{2\lambda+1} | \lambda = 0, \ldots, 3\}$ denote the positions of eight point vortices with positive unit strength $\Gamma_{2\lambda} = 1$ and negative unit strength $\Gamma_{2\lambda+1} = -1$ respectively. When we set the point vortex ζ_0 in the subregion D_0, the locations of the other point vortices are automatically determined so that they satisfy the folding symmetry as in Figure 11(b). As a result, each point vortex ζ_λ is assigned to the subdomain D_λ as we see in Figure 11(a).

Generally, for $N = 2M = 2^K$, if a circular domain can be divided into N subdomains by folding it K times in the same way, we can arrange M point vortices with the positive unit strength and M point vortices with the negative unit strength in the subdomains according to the folding symmetry. Then we say that the circular domain has the *K-folding symmetry* and the folding operation is referred to as the *K-folding transformation*. The configuration of the M positive point vortices $\zeta_{2\lambda}$ and the M negative point vortices $\zeta_{2\lambda+1}$ in the circular domains with the K-folding symmetry is specified by

$$\zeta_{2\lambda} = s^\lambda \zeta_0, \qquad \zeta_{2\lambda+1} = \left(s^\lambda \zeta_0\right)^*, \qquad \lambda = 0, \ldots, M-1, \tag{17}$$

in which s is the same as what we have used in the previous section, i.e., $s = \exp(\mathrm{i}\theta_M)$ with $\theta_M = 2\pi/M$.

Here, we explain how to construct circular domains with the folding symmetry. Let us put D circular obstacles $C_0^{(d)}$ inside the unit circle, whose centers are located at $\delta_0^{(d)}$ and radii are given by $q_0^{(d)}$ for $d = 0, \ldots, D-1$. Then for each obstacle $C_0^{(d)}$, we arrange the other $N = 2M = 2^K$ obstacles according to the K-folding symmetry. Namely, the centers of the obstacles $\left\{C_{2\lambda}^{(d)}, C_{2\lambda+1}^{(d)} | \lambda = 0, \ldots, M-1\right\}$ are given by $\delta_{2\lambda}^{(d)} = s^\lambda \delta_0^{(d)}$ and $\delta_{2\lambda+1}^{(d)} = \left(\delta_{2\lambda}^{(d)}\right)^*$ and their radii

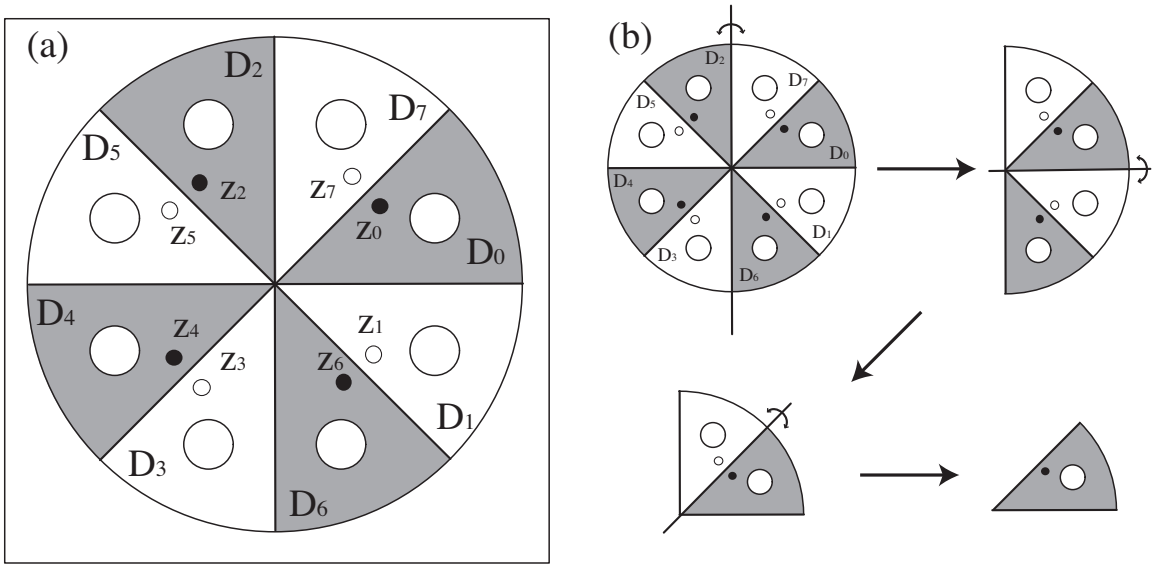

Figure 11: (a) A schematic picture of a circular domain with the folding symmetry. When we put a point vortex with the positive unit strength, depicted as a black solid circle, in the gray region D_0, then the other point vortices with the positive unit strength are assigned to the gray regions, while the point vortices with the negative unit strength, depicted as white small circles, are set in the white regions so that the configuration satisfies the folding symmetry as shown in (b).

are $q_{2\lambda}^{(d)} = q_{2\lambda+1}^{(d)} = q_0^{(d)}$. Consequently, we obtain the circular domain with the $N \times D$ obstacles that is invariant with respect to the K-folding transformation. Examples of the circular domains with the 2-folding symmetry are shown in Figure 12. We note that it is possible to construct the circular domains with the folding symmetry in the annulus as in Figure 12(b).

4.2 Invariance with respect to the K-folding transformation

We show that the relation (17) remains unchanged throughout the evolution when the circular domain is invariant with respect to the folding transformation. We first prove it fo a special circular domain for $D = 1$, say $\mathcal{D}_f$, that contains $N = 2M = 2^K$ identical obstacles. Owing to the K-folding symmetry, the centers and the radii of the obstacles are denoted by $\delta_{2\lambda} = s^\lambda \delta_0$ and $q_{2\lambda} = r$ for $C_{2\lambda}$, and $\delta_{2\lambda+1} = \left(s^\lambda \delta_0\right)^* = (\delta_{2\lambda})^*$ and $q_{2\lambda+1} = r$ for $C_{2\lambda+1}$. The generating functions for the Schottky group associated with the domain $\mathcal{D}_f$ are given by

$$\vartheta_{2\lambda}(\zeta) = \frac{s^\lambda \delta_0 + (r^2 - |\delta_0|^2)\zeta}{1 - s^{-\lambda}\delta_0^* \zeta}, \qquad \vartheta_{2\lambda+1}(\zeta) = \frac{s^{-\lambda}\delta_0^* + (r^2 - |\delta_0|^2)\zeta}{1 - s^\lambda \delta_0 \zeta}.$$

Then we have the following proposition.

Proposition 4.1 *Let $N = 2M = 2^K$ and $s = \exp(2\pi \mathrm{i}/M)$. The positions of point vortices with the positive unit strength and the negative unit strength at time t in the circular domain $\mathcal{D}_f$ are denoted by $\zeta_{2\lambda}(t)$ and $\zeta_{2\lambda+1}(t)$ for $\lambda = 0, \ldots, M-1$ respectively. Then we have $\zeta_{2\lambda}(t) = (\zeta_{2\lambda+1})^*(t) = s^\lambda \zeta_0(t)$ for all time, if it is satisfied at $t = 0$.*

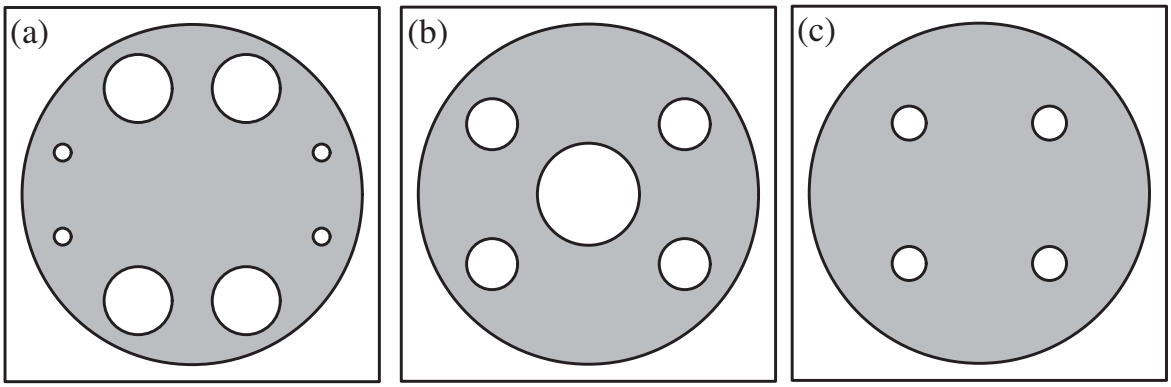

Figure 12: Examples of circular domains that are invariant with respect to the 2-folding transformation for (a) $D = 2$ inside the unit circle and (b) $D = 1$ inside the annulus. (c) The rotationally symmetric circular domain $\mathcal{D}_s$ with four obstacles is also invariant with respect to the 2-folding symmetry.

Proof: We first show that $(\zeta_{2\lambda})^* = \zeta_{2\lambda+1}$ holds for all time. Separating the interactions between the point vortices with the positive and negative strengths, and assuming that $\zeta^*_{2\lambda} = \zeta_{2\lambda+1}$, we have

$$\begin{aligned}
\dot{\zeta}^*_{2\lambda+1} - \dot{\zeta}_{2\lambda} \quad = \quad & -\frac{\mathrm{i}}{2\pi}\sum_{\alpha\neq\lambda}^{M-1}\left\{\left(\frac{\omega^*_\zeta(\zeta_{2\lambda},\zeta_{2\alpha})}{\omega^*(\zeta_{2\lambda},\zeta_{2\alpha})} - \frac{\omega_\zeta(\zeta_{2\lambda},\zeta_{2\alpha})}{\omega(\zeta_{2\lambda},\zeta_{2\alpha})}\right) - \left(\frac{\omega^*_\zeta(\zeta_{2\lambda},\zeta^{*-1}_{2\alpha})}{\omega^*(\zeta_{2\lambda},\zeta^{*-1}_{2\alpha})} - \frac{\omega_\zeta(\zeta_{2\lambda},\zeta^{*-1}_{2\alpha})}{\omega(\zeta_{2\lambda},\zeta^{*-1}_{2\alpha})}\right)\right\} \\
& +\frac{\mathrm{i}}{2\pi}\sum_{\alpha=0}^{M-1}\left\{\left(\frac{\omega^*_\zeta(\zeta_{2\lambda},\zeta^{*}_{2\alpha})}{\omega^*(\zeta_{2\lambda},\zeta^{*}_{2\alpha})} - \frac{\omega_\zeta(\zeta_{2\lambda},\zeta^{*}_{2\alpha})}{\omega(\zeta_{2\lambda},\zeta^{*}_{2\alpha})}\right) - \left(\frac{\omega^*_\zeta(\zeta_{2\lambda},\zeta^{-1}_{2\alpha})}{\omega^*(\zeta_{2\lambda},\zeta^{-1}_{2\alpha})} - \frac{\omega_\zeta(\zeta_{2\lambda},\zeta^{-1}_{2\alpha})}{\omega(\zeta_{2\lambda},\zeta^{-1}_{2\alpha})}\right)\right\} \\
& +\frac{\mathrm{i}}{2\pi}\left(\frac{\omega^*_\zeta(\zeta_{2\lambda},\zeta^{*-1}_{2\lambda})}{\omega^*(\zeta_{2\lambda},\zeta^{*-1}_{2\lambda})} - \frac{\omega_\zeta(\zeta_{2\lambda},\zeta^{*-1}_{2\lambda})}{\omega(\zeta_{2\lambda},\zeta^{*-1}_{2\lambda})}\right).
\end{aligned}$$

This certainly vanishes, if

$$\left(\frac{\omega_\zeta(\zeta,\alpha)}{\omega(\zeta,\alpha)}\right)^* = \frac{\omega_\zeta(\zeta^*,\alpha^*)}{\omega(\zeta^*,\alpha^*)}$$

is satisfied for arbitrary ζ and α in $\mathcal{D}_f$, which is confirmed by using (7). It is easy to see that the first term of (7) always satisfies the condition,

$$\left(\frac{1}{\zeta-\alpha}\right)^* = \frac{1}{\zeta^*-\alpha^*}.$$

Regarding the second term, it is required to show that

$$\left(\sum_{\theta_{\boldsymbol{j}}\in\Theta''}\frac{\theta'_{\boldsymbol{j}}(\zeta)(\alpha-\zeta)}{(\theta_{\boldsymbol{j}}(\zeta)-\alpha)(\theta_{\boldsymbol{j}}(\zeta)-\zeta)}\right)^* = \sum_{\theta_{\boldsymbol{i}}\in\Theta''}\frac{\theta'_{\boldsymbol{i}}(\zeta^*)(\alpha^*-\zeta^*)}{(\theta_{\boldsymbol{i}}(\zeta^*)-\alpha^*)(\theta_{\boldsymbol{i}}(\zeta^*)-\zeta^*)}.$$

This holds true, if there exists a bijection $\boldsymbol{c} : \boldsymbol{j} \mapsto \boldsymbol{i}$ for the word of the map $\theta_{\boldsymbol{j}} \in \Theta''$ such that

$$(\theta_{\boldsymbol{j}}(\zeta))^* = \theta^*_{\boldsymbol{j}}(\zeta^*) = \theta_{\boldsymbol{c}(\boldsymbol{j})}(\zeta^*).$$

The generating function for the Schottky group associated with the domain $\mathcal{D}_f$ satisfies

$$\vartheta_{2\lambda}(\zeta^*) = \frac{s^\lambda \delta_0 + (r^2 - |\delta_0|^2)\zeta^*}{1 - s^{-\lambda}\delta_0^*\zeta^*} = \left(\frac{s^{-\lambda}\delta_0^* + (r^2 - |\delta_0|^2)\zeta}{1 - s^\lambda \delta_0 \zeta}\right)^* = (\vartheta_{2\lambda+1}(\zeta))^* .$$

Therefore, when we introduce a permutation between the labels for the generating functions as

$$c : \begin{pmatrix} 0 & 1 & \cdots & 2\lambda & 2\lambda+1 & \cdots & 2M-2 & 2M-1 \\ 1 & 0 & \cdots & 2\lambda+1 & 2\lambda & \cdots & 2M-1 & 2M-2 \end{pmatrix}, \tag{18}$$

it gives rise to a bijection on the level-one maps of the Schottky group. As for the level-l maps $\theta_{\boldsymbol{j}} \in \Theta''$ with the word $\boldsymbol{j} = (j(1), j(2), \ldots, j(l))$, we define the permutation of the word $\boldsymbol{c}_l$ by

$$\boldsymbol{c}_l(\boldsymbol{j}) = (c(j(1)), c(j(2)), \ldots, c(j(l))),$$

which induces a bijection on the set of the equivalence class of the level-l maps in the Schottky group. Thus $\{\theta_{\boldsymbol{j}}\} = \{\theta_{\boldsymbol{c}_l(\boldsymbol{j})}\}$. In addition, we have $(\theta_{\boldsymbol{j}}(\zeta))^* = \theta_{\boldsymbol{c}_l(\boldsymbol{j})}(\zeta^*)$ and $(\theta'_{\boldsymbol{j}}(\zeta))^* = \theta'_{\boldsymbol{c}_l(\boldsymbol{j})}(\zeta^*)$, since

$$\begin{aligned} (\theta_{\boldsymbol{j}}(\zeta))^* &= (\theta_{j(1)} \circ \theta_{j(2)} \circ \cdots \circ \theta_{j(l)}(\zeta))^* \\ &= \theta_{c(j(1))}((\theta_{j(2)} \circ \cdots \circ \theta_{j(l)}(\zeta))^*) \\ &\cdots \\ &= \theta_{c(j(1))} \circ \theta_{c(j(2))} \circ \cdots \circ \theta_{c(j(l))}(\zeta^*) = \theta_{\boldsymbol{c}_l(\boldsymbol{j})}(\zeta^*). \end{aligned}$$

These relations hold for arbitrary l. Hence, when we define

$$\{\theta_{\boldsymbol{c}(\boldsymbol{j})}\} \equiv \bigcup_{l=1}^{\infty} \{\theta_{\boldsymbol{c}_l(\boldsymbol{j})}\},$$

we have $\{\theta_{\boldsymbol{j}}\} = \{\theta_{\boldsymbol{c}(\boldsymbol{j})}\} = \Theta''$, $(\theta_{\boldsymbol{j}}(\zeta))^* = \theta_{\boldsymbol{c}(\boldsymbol{j})}(\zeta^*)$ and $(\theta'_{\boldsymbol{j}}(\zeta))^* = \theta'_{\boldsymbol{c}(\boldsymbol{j})}(\zeta^*)$ as we have discussed in §3.2. Accordingly, we finally have

$$\left(\sum_{\theta_{\boldsymbol{j}} \in \Theta''} \frac{\theta'_{\boldsymbol{j}}(\zeta)(\alpha - \zeta)}{(\theta_{\boldsymbol{j}}(\zeta) - \alpha)(\theta_{\boldsymbol{j}}(\zeta) - \zeta)}\right)^* = \sum_{\theta_{\boldsymbol{c}(\boldsymbol{j})} \in \Theta''} \frac{\theta'_{\boldsymbol{c}(\boldsymbol{j})}(\zeta^*)(\alpha^* - \zeta^*)}{(\theta_{\boldsymbol{c}(\boldsymbol{j})}(\zeta^*) - \alpha^*)(\theta_{\boldsymbol{c}(\boldsymbol{j})}(\zeta^*) - \zeta^*)}.$$

With the permutation map $\boldsymbol{c}$ for the word of the maps in Θ'', we similarly show that the third term of (7) satisfies

$$\left(\sum_{\theta_{\boldsymbol{j}} \in \Theta''} \frac{\theta_{\boldsymbol{j}}(\alpha) - \theta_{\boldsymbol{j}}(\zeta)}{(\theta_{\boldsymbol{j}}(\alpha) - \zeta)(\theta_{\boldsymbol{j}}(\zeta) - \zeta)}\right)^* = \sum_{\theta_{\boldsymbol{c}(\boldsymbol{j})} \in \Theta''} \frac{\theta_{\boldsymbol{c}(\boldsymbol{j})}(\alpha^*) - \theta_{\boldsymbol{c}(\boldsymbol{j})}(\zeta^*)}{(\theta_{\boldsymbol{c}(\boldsymbol{j})}(\alpha^*) - \zeta^*)(\theta_{\boldsymbol{c}(\boldsymbol{j})}(\zeta^*) - \zeta^*)},$$

which concludes that $(\zeta_{2\lambda}(t))^* = \zeta_{2\lambda+1}(t)$ for all $t \geq 0$, if it is satisfied initially.

Substituting $\zeta_{2\lambda} = (\zeta_{2\lambda+1})^*$ into the equation (6), we have the following reduced equation for the point vortex $\zeta_{2\lambda}$ with the positive unit strength:

$$\begin{aligned} \frac{d\zeta_{2\lambda}}{dt} &= \frac{\mathrm{i}}{2\pi} \sum_{\alpha \neq \lambda}^{M-1} \left(\frac{\omega_\zeta^*(\zeta_{2\lambda}^*, \zeta_{2\alpha}^*)}{\omega^*(\zeta_{2\lambda}^*, \zeta_{2\alpha}^*)} - \frac{\omega_\zeta^*(\zeta_{2\lambda}^*, \zeta_{2\alpha}^{-1})}{\omega^*(\zeta_{2\lambda}^*, \zeta_{2\alpha}^{-1})} \right) - \frac{\mathrm{i}}{2\pi} \sum_{\alpha=0}^{M-1} \left(\frac{\omega_\zeta^*(\zeta_{2\lambda}^*, \zeta_{2\alpha})}{\omega^*(\zeta_{2\lambda}^*, \zeta_{2\alpha})} - \frac{\omega_\zeta^*(\zeta_{2\lambda}^*, \zeta_{2\alpha}^{*-1})}{\omega^*(\zeta_{2\lambda}^*, \zeta_{2\alpha}^{*-1})} \right) \\ &\quad - \frac{\mathrm{i}}{2\pi} \frac{\omega_\zeta^*(\zeta_{2\lambda}^*, \zeta_{2\lambda}^{-1})}{\omega^*(\zeta_{2\lambda}^*, \zeta_{2\lambda}^{-1})}. \end{aligned}$$

All we have to show is that $\zeta_{2\lambda}(t) = s^\lambda \zeta_0(t)$ holds for all time. It can be done in the similar manner as in Proposition 3.1, since the reduced system is invariant with respect to the rotation around the origin by the degree θ_M. Thus the proof is finished.

□

For general circular domains with the folding symmetry, we obtain the same result by modifying the proof slightly.

Theorem 4.1 *Let $N = 2M = 2^K$ and $s = \exp(2\pi \mathrm{i}/M)$. Suppose that the circular domain is invariant with respect to the K-folding transformation, in which the point vortices with the positive unit strength and the negative unit strength at time t are located at $\zeta_{2\lambda}(t)$ and $\zeta_{2\lambda+1}(t)$ for $\lambda = 0, \ldots, M-1$ respectively. Then we have $\zeta_{2\lambda} = (\zeta_{2\lambda+1})^* = s^\lambda \zeta_0$ for all time, if it is satisfied initially.*

Proof: Following the proof of Proposition 4.1, we first show the relation $(\zeta_{2\lambda})^* = \zeta_{2\lambda+1}$ holds for all time, if it is satisfied at the initial moment. The only difference is the definition of the permutation of the label c for the generating functions of the Schottky group. Instead of (18), we introduce

$$c : \begin{pmatrix} 0 & 1 & \cdots & 2\lambda & 2\lambda+1 & \cdots & 2DM-2 & 2DM-1 \\ 1 & 0 & \cdots & 2\lambda+1 & 2\lambda & \cdots & 2DM-1 & 2DM-2 \end{pmatrix},$$

for the circular domains with the K-folding symmetry in the unit circle, and

$$c : \begin{pmatrix} 0 & 1 & \cdots & 2\lambda & 2\lambda+1 & \cdots & 2DM-2 & 2DM-1 & 2DM \\ 1 & 0 & \cdots & 2\lambda+1 & 2\lambda & \cdots & 2DM-1 & 2DM-2 & 2DM \end{pmatrix},$$

for those in the annulus. Since both of the permutations induce a bijection $\boldsymbol{c}$ on the set Θ'' of the equivalence class such that $(\theta_{\boldsymbol{j}}(\zeta))^* = \theta_{\boldsymbol{c}(\boldsymbol{j})}(\zeta^*)$ and $(\theta_{\boldsymbol{j}}(\zeta)')^* = \theta'_{\boldsymbol{c}(\boldsymbol{j})}(\zeta^*)$, we have $(\zeta_{2\lambda})^* = \zeta_{2\lambda+1}$.

Then we reduce the equation of motion (6) to that for the point vortices with the positive strength by using $(\zeta_{2\lambda})^* = \zeta_{2\lambda+1}$. The invariance of the reduced system in terms of the rotation by the degree θ_M is proved in the same way as in Theorem 3.1.

□

4.3 Fixed equilibria with the folding symmetry

Owing to Theorem 4.1, the dynamics of the N point vortices with the opposite signs is reduced to a one-degree-of-freedom integrable Hamiltonian dynamical system, whose Hamiltonian is given by

$$\begin{aligned} H_f^{(\zeta)}(\zeta_0) \;=\; & \sum_{\lambda=0}^{M-1} \sum_{\alpha=\lambda+1}^{M-1} G(s^\lambda \zeta_0; s^\alpha \zeta_0) + G((s^\lambda \zeta_0)^*; (s^\alpha \zeta_0)^*) - \sum_{\lambda=0}^{M-1} \sum_{\alpha=\lambda}^{M-1} G(s^\lambda \zeta_0; (s^\alpha \zeta_0)^*) \\ & -\frac{1}{2} \sum_{\lambda=0}^{M-1} R(s^\lambda \zeta_0; (s^\lambda \zeta_0)^*) + R((s^\lambda \zeta_0)^*; (s^\lambda \zeta_0)^*). \end{aligned} \tag{19}$$

For the circular domains with the 1-folding symmetry, we have fixed configurations of the vortex dipole, which has been investigated in the paper [18]. Hence we consider the circular domains that are invariant with respect to the 2-folding transformation. Figure 13 shows the contour lines of the reduced Hamiltonian (19) for the circular domains given in Figure 12. Fixed configurations

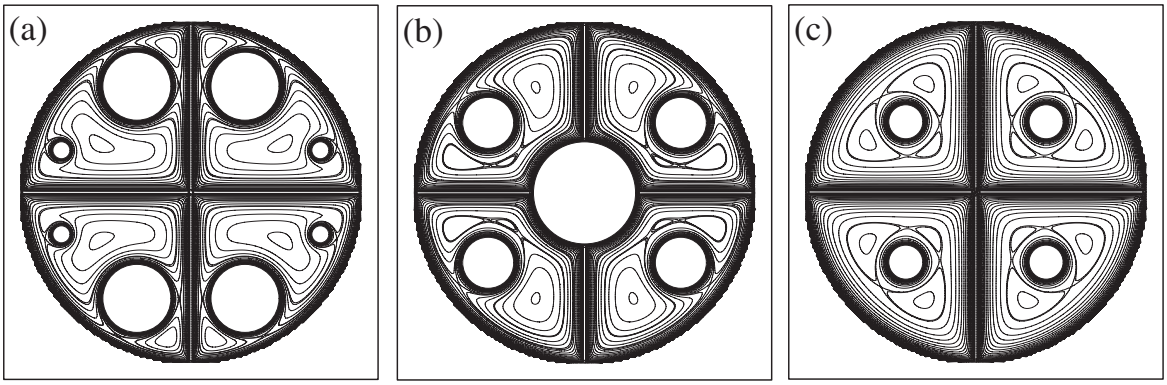

Figure 13: Contour plots of the Hamiltonian (19) for the circular domains with the 2-folding symmetry corresponding to those in Figure 12. The saddles and centers represent the locations of fixed equilibria of four point vortices.

correspond to saddles and centers of the contour lines, in which the point vortices with the positive strength and the negative strength are arranged alternately at the vertices of a rectangle as in Figure 14(b). We refer to this configuration as the *alternate rectangle*. When the four point vortices are at the vertices of a square, we particularly call it the *alternate* 4-*ring*. See Figure 14(a). The alternate 4-rings are observed in the rotationally symmetric circular domain $\mathcal{D}_s$ of Figure 13(c).

In what follows, we investigate fixed equilibria in the circular domain $\mathcal{D}_s$ with four obstacles, which is invariant with respect to not only the rotation but also the 2-folding transformation. Figure 15 shows the contour plots of the Hamiltonian (19) in $\mathcal{D}_s$ for various a with the fixed radius $r = 0.1$. We also give a schematic picture of the topological pattern for each of the contour plot in the quadrant of the unit circle. In Figure 15(a) for $a = 0.4$, there are two centers that corresponds to the alternate 4-rings and two saddles of the alternate rectangles between the obstacles. The saddles are connected by heteroclinic orbits. We refer to this topological pattern as Type-I. When $a = 0.5$ in Figure 15(b), one of the alternate 4-ring becomes a saddle with homoclinic connections, in which two centers of the alternate rectangles are surrounded. This is called Type-II. For $a = 0.6$, the number of the fixed configurations remains the same, but the topological structure of the separatrices changes. This is Type-III. Finally, when $a = 0.7$, there is no alternate rectangle, while we still observe a center and a saddle of the 4-rings, which is Type-IV.

For various a and r, we observe the four topological patterns of the contour lines given in Figure 15, which are classified in Table 1. Note that the range of the radius r depends on a, namely $0 < r < \min(a \sin(\pi/4), 1 - a)$. When r is sufficiently small, we have Type-IV pattern. For larger a, we observe Type-IV, while Type-I for smaller a. Type-II and Type-III patterns are typically observed for $a = 0.5$ and $a = 0.6$ respectively. Figure 16 gives a schematic diagram describing how the topological patterns change due to bifurcations of the fixed equilibria and a global transition of the separatrices. The transition from Type-IV to Type-I occurs when the unstable alternate 4-ring becomes neutrally stable and new unstable alternate rectangles with heteroclinic connections appear. When one of the neutrally stable alternate 4-rings in Type-I pattern becomes unstable, the topological pattern changes to Type-II. A degenerate pinching bifurcation of the neutrally stable 4-ring gives rise to two unstable and two neutrally stable alternate rectangles, which results in the transition from Type-IV to Type-III. Finally, the route from Type-II to Type-III is allowed due to a global reconnection of separatrices through a non-generic contour pattern, depicted as

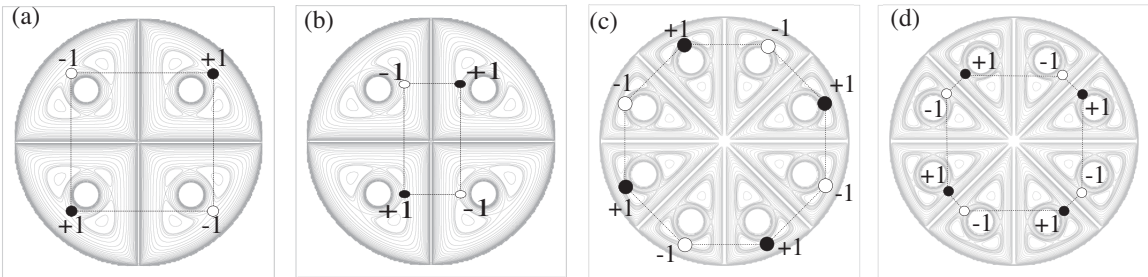

Figure 14: A catalogue of fixed point equilibria in the circular domains with the folding symmetry. (a) An alternate 4-ring and (b) an alternate rectangle; (c) An alternate 8-ring and (b) an alternate octagon.

Type-V in Figure 16. As a matter of fact, Figure 13(c) is an example of such Type-V pattern. Let us remark that it is possible to consider another route from Type-IV to Type-II through Type VI as shown in Figure 16, but we hardly observe Type-VI pattern. Let us note the existence of relative equilibria. The topological structure of the contour lines indicates that the relative distances of the point vortices change unless they are the fixed configurations, which means there is no relative equilibrium in the circular domains with the folding symmetry.

Some more examples of the contour plots of the Hamiltonian (19) for $\mathcal{D}_s$ with eight obstacles are given in Figures 17(a) and (b). The radius of the obstacle is $r = 0.1$ and we change a. In both cases, we find a center and a saddle of the alternate 8-rings, in which the point vortices with the positive and negative strengths are placed at the vertices of a regular octagon as we see in Figure 14(c). As the obstacles approach the origin, the stability of the alternate 8-ring remains the same, but there emerge four fixed equilibria, two saddles and two centers, in which the positive and the negative point vortices are arranged alternately along the vertices of a octagon. A schematic picture for the alternate octagon is shown in Figure 14(d).

5 Fixed equilibria in general symmetric multiply connected domains

5.1 Equation of motion for N point vortices in general domains

We consider multiply connected domains that are not circular domains. As we have mentioned in the introduction, for an arbitrary multiply connected domain with M holes in the complex z-plane, say $\mathcal{D}_z$, there exists a conformal mapping $\zeta = f(z)$ that maps $\mathcal{D}_z$ to a circular domain with M circular obstacles $\mathcal{D}_\zeta$ in the complex ζ-plane[15].

Let $\{z_\lambda(t)|\lambda = 0, \ldots, M-1\}$ denote the positions of the point vortices in $\mathcal{D}_z$ with the strengths $\{\Gamma_\lambda|\lambda = 0, \ldots, M-1\}$. The Kirchhoff-Routh path function $H^{(z)}$ for the M point vortices is

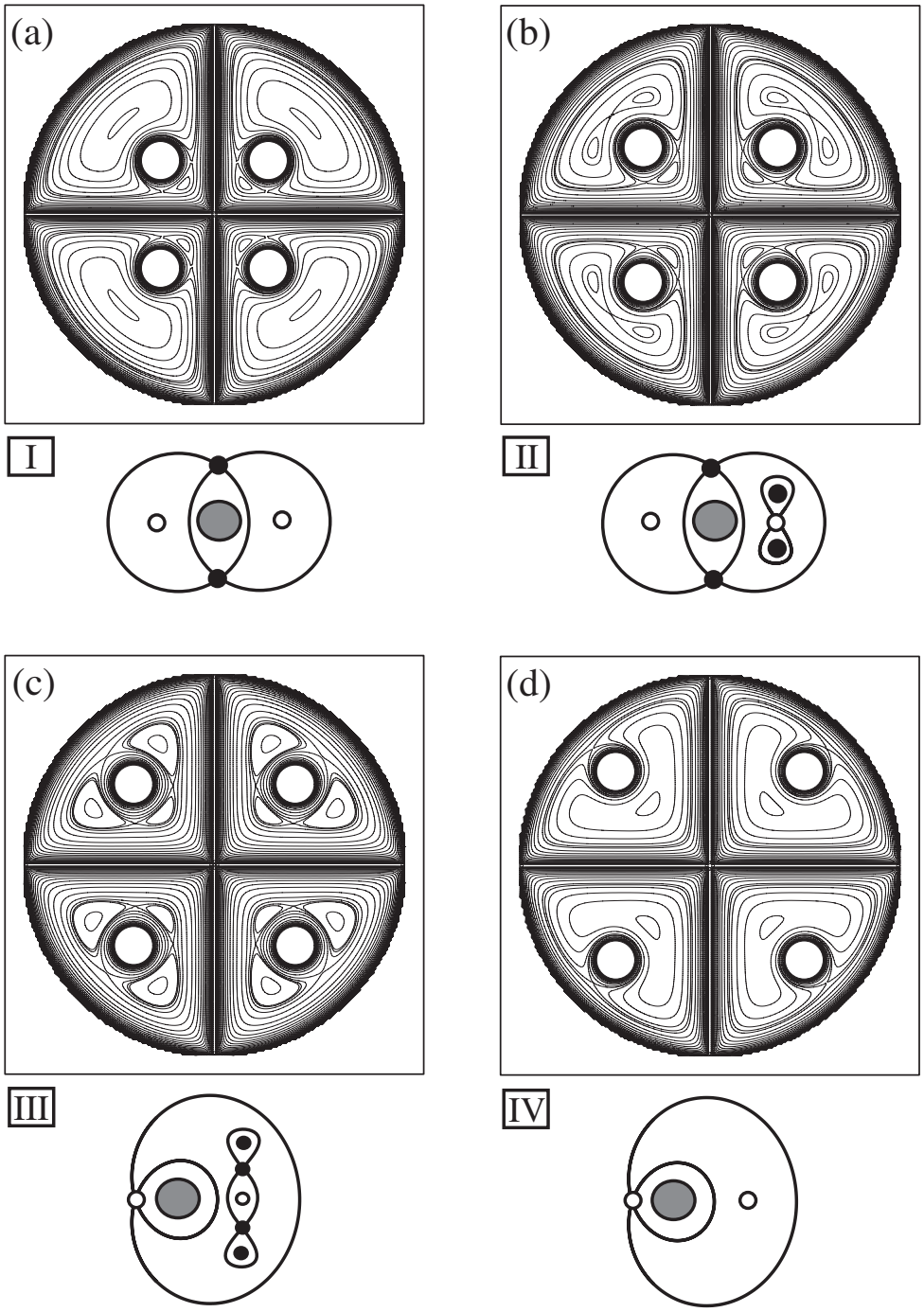

Figure 15: Contour plots of the Hamiltonian (19) in $\mathcal{D}_s$ for $N = 4$ and the corresponding topological structures of the contour lines in the quadrant of the unit circle for (a) $a = 0.4$ and $r = 0.1$; (b) $a = 0.5$ and $r = 0.1$; (c) $a = 0.6$ and $r = 0.1$; (d) $a = 0.7$ and $r = 0.1$. In the schematic pictures of the topological structures, the big gray solid circle represents the obstacle, the white and the black small circles symbolize the alternate 4-rings and the alternate rectangles respectively.

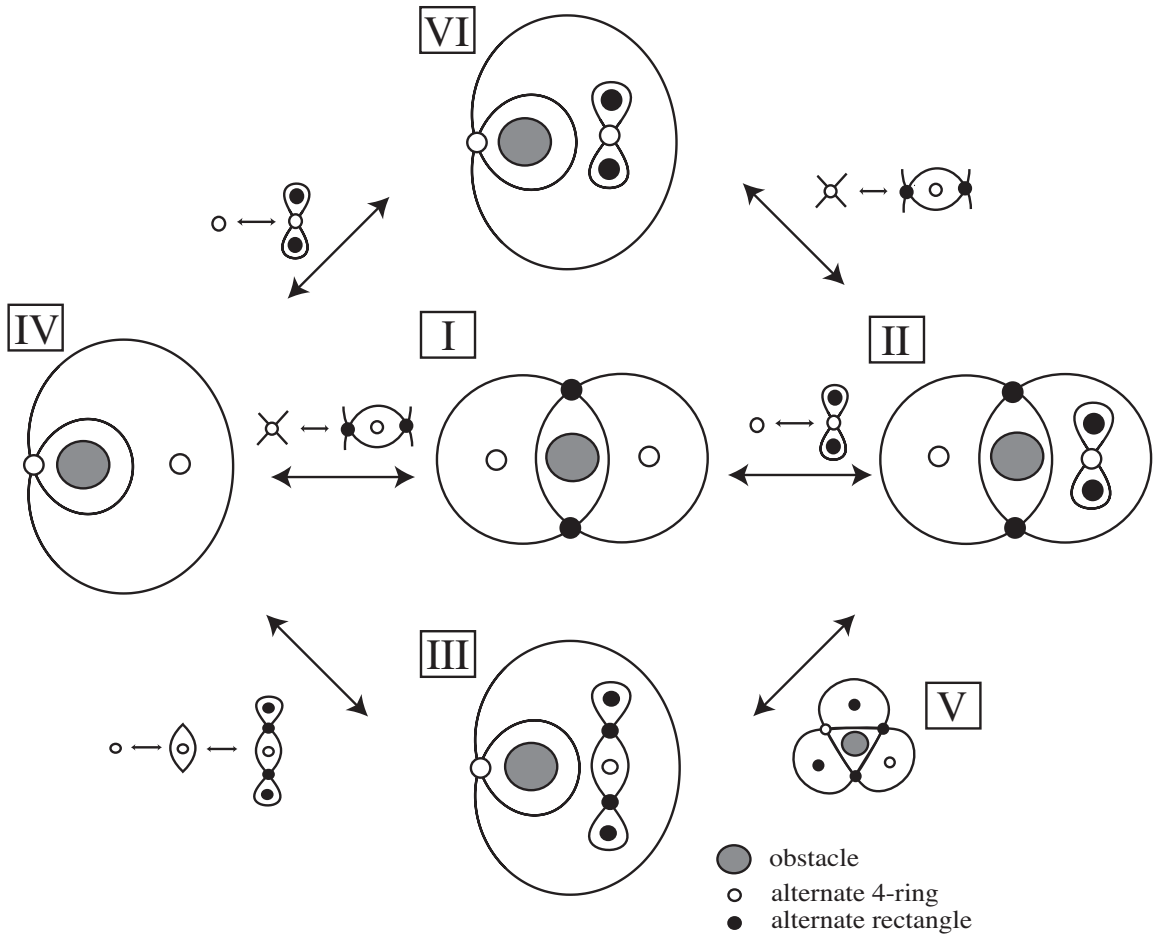

Figure 16: Transitions between the topological patterns of the contour lines of the Hamiltonian in the quadrant of the multiply connected circular domain $\mathcal{D}_s$. The big gray circle represents a circular obstacle in the quadrant, and the white and black circles symbolize alternate 4-rings and alternate rectangles respectively. When the transition occurs, we observe either a change of stability of an equilibrium or a change of global toplogical structure of separatrices.

$a \setminus r$	0.02	0.05	0.1	0.15	0.2	0.25	0.3	0.35
0.1	IV	I						
0.2	IV	I	I					
0.3	IV	I	I	I	II			
0.4	IV	I	I	II	II	II		
0.5	IV	II	II	II	II	II	II	
0.6	III	III	III	III	III	III	III	III
0.7	IV	IV	IV	III	III	III		
0.8	IV	IV	IV	IV				
0.9	IV	IV						

Table 1: Classification of the topological patterns of the contour lines of the Hamiltonian (19) with $N = 4$ observed for various a and r. The symbols I-IV represent the topological patterns of the contour lines in the quadrant of the circular domain, whose schematic pictures are shown in Figure 15.

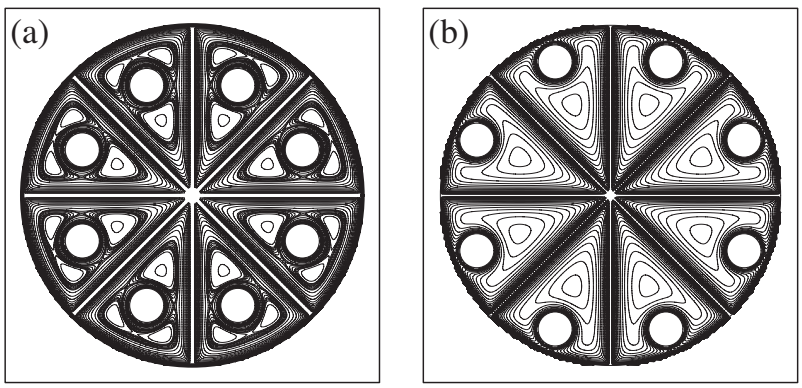

Figure 17: Contour plots of the Hamiltonian (19) in $\mathcal{D}_s$ with eight obstacles for (a) $a = 0.7$ and $r = 0.1$; (b) $a = 0.85$ and $r = 0.1$. The saddles and centers represent the locations of fixed equilibria of eight point vortices.

obtained from $H^{(\zeta)}$ as follows:

$$H^{(z)}(z_0, z_0^*, \ldots, z_{N-1}, z_{N-1}^*) = H^{(\zeta)}(\zeta_0, \zeta_0^*, \ldots, \zeta_{N-1}, \zeta_{N-1}^*) - \sum_{\lambda=0}^{N-1} \frac{\Gamma_\lambda^2}{4\pi} \log |f_z(z_\lambda)|,$$

in which $\zeta_\lambda = f(z_\lambda)$ denotes the position of the point vortex in $\mathcal{D}_\zeta$ mapped by the conformal mapping. The equation of motion for the N point vortices in $\mathcal{D}_z$ is derived from $H^{(z)}$ with the chain rule:

$$\begin{aligned}
\frac{dz_\lambda}{dt} = -\frac{2\mathrm{i}}{\Gamma_\lambda}\frac{\partial H^{(z)}}{\partial z_\lambda^*} &= -\frac{2\mathrm{i}}{\Gamma_\lambda}\left(\frac{\partial H^{(\zeta)}}{\partial \zeta_\lambda} f_z(z_\lambda) - \frac{\Gamma_\lambda^2}{8\pi}\frac{f_{zz}(z_\lambda)}{f_z(z_\lambda)}\right)^* \\
&= -\frac{2\mathrm{i}}{\Gamma_\lambda}\frac{\partial H^{(\zeta)}}{\partial \zeta_\lambda^*} f_z^*(z_\lambda^*) + \mathrm{i}\frac{\Gamma_\lambda}{4\pi}\frac{f_{zz}^*(z_\lambda^*)}{f_z^*(z_\lambda^*)} \\
&= \frac{d\zeta_\lambda}{dt} f_z^*(z_\lambda^*) + \mathrm{i}\frac{\Gamma_\lambda}{4\pi}\frac{f_{zz}^*(z_\lambda^*)}{f_z^*(z_\lambda^*)}. \qquad (20)
\end{aligned}$$

Therefore, even if a configuration of the point vortices $\{z_\lambda | \lambda = 0, \ldots, M-1\}$ becomes a fixed equilibrium in $\mathcal{D}_z$, the mapped point vortices $\{\zeta_\lambda | \lambda = 0, \ldots, M-1\}$ does not necessarily give a stationary configuration in $\mathcal{D}_\zeta$, since the additional term $f_{zz}(z_\lambda)/f_z(z_\lambda)$ in the equation (20) is not always zero for all conformal mappings. In other words, fixed equilibria are not invariant with respect to the conformal mapping. In the following subsections, we consider a sufficient condition for the conformal mapping that makes fixed equilibria conformally invariant when the domain has the rotational symmetry and/or the folding symmetry.

5.2 Domains with the rotational symmetry

A multiply connected domain $\mathcal{D}_z$ is said to be symmetric with respect to the rotation around the origin by the degree $\theta_M = 2\pi/M$, if and only if

$$\forall z \in \mathcal{D}_z \Longrightarrow s^\lambda z \in \mathcal{D}_z,$$

where $s = \exp(\mathrm{i}\theta_M)$. Suppose that the conformal mapping $\zeta = f(z)$ from $\mathcal{D}_z$ to a circular domain satisfies

$$f(s^\lambda z) = s^\lambda f(z), \quad \forall z \in \mathcal{D}_z, \qquad (21)$$

then the circular domain $\mathcal{D}_\zeta$ is rotationally symmetric, since there exists a point $z \in \mathcal{D}_z$ such that $s^\lambda \zeta = s^\lambda f(z) = f(s^\lambda z) \in \mathcal{D}_\zeta$ due to $s^\lambda z \in \mathcal{D}_z$ for arbitrary $\zeta \in \mathcal{D}_\zeta$. Then we show the following theorem.

Theorem 5.1 *Suppose that the multiply connected domain $\mathcal{D}_z$ is invariant with respect to the rotation around the origin by the degree $\theta_M = 2\pi/M$ and the conformal mapping $f(z)$ from $\mathcal{D}_z$ to a circular domain satisfies (21). Let $\{z_\lambda(t) \in \mathcal{D}_z | \lambda = 0, \ldots, M-1\}$ denote the positions of the point vortices with the unit strength at time t. Then, if $z_\lambda(0) = s^\lambda z_0(0)$ holds, then we have $z_\lambda(t) = s^\lambda z_0(t)$ for $t \geq 0$.*

Proof: It follows from (21) that we have

$$f_z(s^\lambda z) = f_z(z), \qquad s^\lambda f_{zz}(s^\lambda z) = f_{zz}(z). \qquad (22)$$

Suppose that $z_\lambda = s^\lambda z_0$, then we have $\zeta_\lambda = f(z_\lambda) = f(s^\lambda z_0) = s^\lambda f(z_0) = s^\lambda \zeta_0$, which yields $\dot{\zeta}_\lambda = s^\lambda \dot{\zeta}_0$ owing to Theorem 3.1. Therefore, we have $\dot{z}_\lambda = s^\lambda \dot{z}_0$, since if follows from (22) and $\dot{\zeta}_\lambda = s^\lambda \dot{\zeta}_0$ that

$$\begin{aligned}
\dot{z}_\lambda - s^\lambda \dot{z}_0 &= \dot{\zeta}_\lambda f_z^*(z_\lambda^*) + \frac{\mathrm{i}}{4\pi}\frac{f_{zz}^*(z_\lambda^*)}{f_z^*(z_\lambda^*)} - s^\lambda \dot{\zeta}_0 f_z^*(z_0^*) - \frac{\mathrm{i}}{4\pi}\frac{s^\lambda f_{zz}^*(z_0^*)}{f_z^*(z_0^*)} \\
&= \dot{\zeta}_\lambda f_z^*((s^\lambda z_0)^*) - s^\lambda \dot{\zeta}_0 f^*(z_0^*) + \frac{\mathrm{i}}{4\pi}\left(\frac{f_{zz}^*((s^\lambda z_0)^*)}{f_z^*((s^\lambda z_0)^*)} - \frac{s^\lambda f_{zz}^*(z_0^*)}{f_z^*(z_0^*)}\right) \\
&= (\dot{\zeta}_\lambda - s^\lambda \dot{\zeta}_0) f^*(z_0^*) = 0.
\end{aligned}$$

□

Thanks to Theorem 5.1, we can reduce the N-vortex system in $\mathcal{D}_z$ to an integrable one-degree-of-freedom Hamiltonian dynamical system. Furthermore, fixed equilibria in $\mathcal{D}_\zeta$ are obtained by mapping fixed equilibria in $\mathcal{D}_\zeta$ with the conformal mapping.

5.3 Domains with the K-folding symmetry

Let us set $N = 2M = 2^K$ and $s = \exp(2\pi \mathrm{i}/M)$. A multiply connected domain $\mathcal{D}_z$ is symmetric with respect to the K-folding transformation, if and only if

$$\forall z \in \mathcal{D}_z \Longrightarrow s^\lambda z, (s^\lambda z)^* \in \mathcal{D}_z.$$

Suppose the conformal mapping $\zeta = f(z)$ from $\mathcal{D}_z$ to a circular domain $\mathcal{D}_\zeta$ satisfies the following relations:

$$f(s^\lambda z) = s^\lambda f(z), \quad f(z) = f^*(z), \quad \forall z \in \mathcal{D}_z. \tag{23}$$

Then the circular domain $\mathcal{D}_\zeta$ is symmetric with respect to the K-folding transformation, since

$$s^\lambda \zeta = s^\lambda f(z) = f(s^\lambda z) \in \mathcal{D}_\zeta, \qquad (s^\lambda z)^* = (f(s^\lambda z))^* = f^*((s^\lambda z)^*) = f((s^\lambda z)^*) \in \mathcal{D}_\zeta.$$

Now we set M point vortices $\{z_{2\lambda} | \lambda = 0, \ldots, M-1\}$ with the positive unit strength $\Gamma_{2\lambda} = 1$ and M point vortices $\{z_{2\lambda+1} | \lambda = 0, \ldots, M-1\}$ with the negative unit strength $\Gamma_{2\lambda+1} = -1$ in $\mathcal{D}_z$. Then we have the following result.

Theorem 5.2 *Let $N = 2M = 2^K$ and $s = \exp(2\pi \mathrm{i}/M)$. Suppose that the multiply connected domain $\mathcal{D}_z$ is invariant with respect to the K-folding transformation and that the conformal mapping $f(z)$ from $\mathcal{D}_z$ to a circular domain satisfies (23). Let the point vortices with the positive unit strength and the negative unit strength at time t be located at $z_{2\lambda}(t)$ and $z_{2\lambda+1}(t)$ for $\lambda = 0, \ldots, M-1$ respectively. Then we have $z_{2\lambda} = (z_{2\lambda+1})^* = s^\lambda z_0$ for all time, if it is satisfied initially.*

Proof: As in the proof of Proposition 4.1 and Theorem 4.1, we first show $\dot{z}_{2\lambda+1} = \dot{z}_{2\lambda}^*$, if $z_{2\lambda+1} = z_{2\lambda}^*$. It follows from (23) that we have

$$f_z(z) = f_z^*(z), \qquad f_{zz}(z) = f_{zz}^*(z), \tag{24}$$

and

$$\zeta_{2\lambda+1} = f(z_{2\lambda+1}) = f^*(z_{2\lambda+1}) = (f(z_{2\lambda}))^* = \zeta_{2\lambda}^*,$$

which yields $\dot{\zeta}_{2\lambda+1} = \dot{\zeta}^*_{2\lambda}$ due to Theorem 4.1. Therefore, noting that $\Gamma_{2\lambda} = 1$ and $\Gamma_{2\lambda+1} = -1$, we obtain

$$\begin{aligned}
\dot{z}_{2\lambda+1} - \dot{z}^*_{2\lambda} &= \dot{\zeta}_{2\lambda+1} f^*_z(z^*_{2\lambda+1}) - \frac{i}{4\pi}\frac{f^*_{zz}(z^*_{2\lambda+1})}{f^*_z(z^*_{2\lambda+1})} - \left(\dot{\zeta}_{2\lambda} f^*_z(z^*_{2\lambda}) + \frac{i}{4\pi}\frac{f^*_{zz}(z^*_{2\lambda})}{f^*_z(z^*_{2\lambda})}\right)^* \\
&= \dot{\zeta}_{2\lambda+1} f^*_z(z_{2\lambda}) - \dot{\zeta}^*_{2\lambda} f_z(z_{2\lambda}) - \frac{i}{4\pi}\left(\frac{f^*_{zz}(z_{2\lambda})}{f^*_z(z_{2\lambda})} - \frac{f_{zz}(z_{2\lambda})}{f_z(z_{2\lambda})}\right),
\end{aligned}$$

which vanishes due to (24) and $\dot{\zeta}_{2\lambda+1} = \dot{\zeta}^*_{2\lambda}$. Thus we have $z_{2\lambda+1} = z^*_{2\lambda}$, with which the equation of motion for the N point vortices is reduced to that for the M point vortices $\{z_{2\lambda} | \lambda = 0, \ldots, M-1\}$. Since the reduced equation is symmetric with respect to the rotation around the origin by the degree $2\pi/M$, we can show $\dot{z}_{2\lambda} = s^\lambda \dot{z}_0$ similarly as in Theorem 5.1.

□

Thus alternate N-gons for the point vortices with the positive strength and the negative strength in the domain $\mathcal{D}_z$ are obtained by mapping fixed equilibria in the circular domain $\mathcal{D}_\zeta$ with the conformal mapping.

5.4 Examples of the conformal mapping

The sufficient conditions (21) and (23) on the conformal mapping guarantee that fixed equilibria in the symmetric circular domains are mapped to those in the multiply connected domains with the same symmetries by the conformal mapping. However, we say nothing about the existence of conformal mappings that satisfy (21) and (23). So we give some non-trivial examples.

We rewrite the sufficient conditions in terms of the inverse of the conformal mapping $z = f^{-1}(\zeta)$. The condition (21) for the rotationally symmetric domains is equivalent to

$$f(s^\lambda z) = s^\lambda(z) \Longleftrightarrow f(s^\lambda f^{-1}(\zeta)) = s^\lambda \zeta \Longleftrightarrow s^\lambda f^{-1}(\zeta) = f^{-1}(s^\lambda \zeta). \tag{25}$$

Regarding the K-folding symmetry, we have

$$f^{-1}(s^\lambda z) = s^\lambda f^{-1}(z), \qquad \big(f^{-1}\big(\zeta)\big)^* = f^{-1}(\zeta^*), \tag{26}$$

since

$$f^*(z) = f(z) \Longleftrightarrow f(z^*) = (f(z))^* = \zeta^* \Longleftrightarrow z^* = f^{-1}(\zeta^*) \Longleftrightarrow (f^{-1}(\zeta))^* = f^{-1}(\zeta^*).$$

Now we show the following lemma for the Schottky-Klein prime function.

Lemma 5.1 *Suppose that the circular domain $\mathcal{D}_\zeta$ is invariant with respect to the rotation around the origin by the degree $2\pi/M$. Then the Schottky-Klein prime function $\omega(\zeta, \alpha)$ associated with $\mathcal{D}_\zeta$ satisfies*

$$\omega(s^\lambda \zeta, s^\lambda \alpha) = s^\lambda \omega(\zeta, \alpha), \tag{27}$$

in which $s = \exp(2\pi \mathrm{i}/M)$.

Proof: Let $\boldsymbol{q} = \boldsymbol{\sigma}^{-\lambda}(\boldsymbol{j})$. Then it follows from Lemma 3.1 that

$$\begin{aligned}\omega'(s^\lambda\zeta, s^\lambda\alpha) &= \prod_{\theta_{\boldsymbol{j}}\in\Theta''} \frac{(\theta_{\boldsymbol{j}}(s^\lambda\zeta) - s^\lambda\alpha)(\theta_{\boldsymbol{j}}(s^\lambda\alpha) - s^\lambda\zeta)}{(\theta_{\boldsymbol{j}}(s^\lambda\zeta) - s^\lambda\zeta)(\theta_{\boldsymbol{j}}(s^\lambda\alpha) - s^\lambda\alpha)} \\ &= \prod_{\theta_{\boldsymbol{j}}\in\Theta''} \frac{(\theta_{\boldsymbol{q}}(\zeta) - \alpha)(\theta_{\boldsymbol{q}}(\alpha) - \zeta)}{(\theta_{\boldsymbol{q}}(\zeta) - \zeta)(\theta_{\boldsymbol{q}}(\alpha) - \alpha)} = \omega'(\zeta, \alpha). \end{aligned} \tag{28}$$

Note that we use the equivalence of the sets $\{\theta_{\boldsymbol{j}}\} = \{\theta_{\boldsymbol{q}}\} = \Theta''$. Hence, we have $\omega(s^\lambda\zeta, s^\lambda\alpha) = (s^\lambda\zeta - s^\lambda\alpha)\omega'(s^\lambda\zeta, s^\lambda\alpha) = s^\lambda(\zeta - \alpha)\omega'(\zeta, \alpha) = s^\lambda\omega(\zeta, \alpha)$.

□

We also have the following lemma for the Schottky-Klein prime function associated with the circular domain with the K-folding symmetry.

Lemma 5.2 *Let $N = 2M = 2^K$ and $s = \exp(2\pi\mathrm{i}/M)$. Suppose that the circular domain is symmetric with respect to the K-folding symmetry. Then the Schottky-Klein prime function associated with the circular domain satisfies*

$$\omega(s^\lambda\zeta, s^\lambda\alpha) = s^\lambda\omega(\zeta, \alpha), \qquad (\omega(\zeta, \alpha))^* = \omega(\zeta^*, \alpha^*). \tag{29}$$

Proof: Since the first part of (29) is similarly shown as in Lemma 5.1, we prove the second part. We must note that the elements of the Schottky group associated with the circular domains with the folding symmetry satisfy $(\theta_{\boldsymbol{j}}(\zeta))^* = \theta_{\boldsymbol{c}(\boldsymbol{j})}(\zeta^*)$ and $(\theta'_{\boldsymbol{j}}(\zeta))^* = \theta'_{\boldsymbol{c}(\boldsymbol{j})}(\zeta^*)$ for the permutation of the word $\boldsymbol{c}$ defined in §4. Then, for $\boldsymbol{q} = \boldsymbol{c}(\boldsymbol{j})$, we have

$$\begin{aligned}(\omega'(\zeta, \alpha))^* &= \left(\prod_{\theta_{\boldsymbol{j}}\in\Theta''} \frac{(\theta_{\boldsymbol{j}}(\zeta) - \alpha)(\theta_{\boldsymbol{j}}(\alpha) - \zeta)}{(\theta_{\boldsymbol{j}}(\zeta) - \zeta)(\theta_{\boldsymbol{j}}(\alpha) - \alpha)}\right)^* \\ &= \prod_{\theta_{\boldsymbol{q}}\in\Theta''} \frac{(\theta_{\boldsymbol{q}}(\zeta^*) - \alpha^*)(\theta_{\boldsymbol{q}}(\alpha^*) - \zeta^*)}{(\theta_{\boldsymbol{q}}(\zeta^*) - \zeta^*)(\theta_{\boldsymbol{q}}(\alpha^*) - \alpha^*)} = \omega'(\zeta^*, \alpha^*), \end{aligned} \tag{30}$$

which yields $\omega^*(\zeta^*, \alpha^*) = ((\zeta - \alpha)\omega'(\zeta, \alpha))^* = (\zeta - \alpha)\omega'(\zeta^*, \alpha^*) = \omega(\zeta^*, \alpha^*)$.

□

These lemmas indicate that the functions $\omega(\zeta, 0)$ and $\omega(\zeta, \infty)$ satisfy (25) and (26). Thus, we can construct many conformal mappings with these functions that satisfy the sufficient conditions, for instance,

$$f(\zeta) = \frac{\zeta^{\beta+1}\omega(\zeta, 0)^{\gamma-\beta}}{\omega(\zeta, \infty)^\gamma}, \qquad \gamma \geq \beta \geq 0.$$

We give two more conformal mappings that satisfy the conditions (25) and (26). The first example is represented by

$$\eta(\zeta) = \frac{\zeta\omega'(\zeta, 0)}{\omega'(\zeta, \infty)}.$$

Crowdy[6] shows that $\eta(\zeta)$ maps the circular domains to the multiply connected domain $\mathcal{D}_\eta$ inside the unit circle with circular slits. Namely, while the boundary of the unit circle $|\zeta| = 1$ is mapped

to that of the unit circle $|\eta| = 1$, the boundaries of the M circular obstacles $\{C_j | j = 0, \ldots, M-1\}$ are mapped to the circular slits

$$|\eta| = r_j < 1, \qquad \arg \eta \in \left[\phi_1^{(j)}, \phi_2^{(j)}\right],$$

for some $\{r_j, \phi_1^{(j)}, \phi_2^{(j)} | j = 0, \ldots, M-1\}$. Note that $\eta(\zeta)$ maps the origin of the circular domain to the origin of $\mathcal{D}_\eta$. The conformal mapping satisfies the sufficient conditions (25) and (26), since it follows from (28) and (30) with $\alpha = 0$ and $\alpha = \infty$ that

$$\eta(s^\lambda \zeta) = \frac{s^\lambda \zeta \omega'(s^\lambda \zeta, 0)}{\omega'(s^\lambda \zeta, \infty)} = \frac{s^\lambda \zeta \omega'(\zeta, 0)}{\omega'(\zeta, \infty)} = s^\lambda \eta(\zeta),$$

and

$$(\eta(\zeta))^* = \frac{\zeta^* \omega'^*(\zeta^*, 0)}{\omega'^*(\zeta^*, \infty)} = \frac{\zeta^* \omega'(\zeta^*, 0)}{\omega'(\zeta^*, \infty)} = \eta(\zeta^*).$$

The second one is a conformal mapping given by Crowdy[9], which is represented by

$$z = g(\zeta) = R\left(\frac{\omega(\zeta, \alpha)\omega(\zeta, \alpha^{-1})}{\omega(\zeta, \beta)\omega(\zeta, \beta^{-1})}\right), \qquad \alpha, \beta, R \in \mathbb{R}. \tag{31}$$

It maps a circular domain with the 1-folding symmetry to an exterior domain with three flat plates with the same symmetry as we see in Figure 18. The unit circle and the two symmetric circular boundaries are mapped to three radial slits whose common center is the origin. The two real points α and β in the complex ζ-plane are mapped to 0 and ∞ of the complex z-plane respectively. The parameter R is a scaling factor. The conformal mapping can be applied to the Kasper wing problem mentioned in the introduction by choosing the parameters α, β, R and the center and the radius of the circular boundaries appropriately. It follows from Lemma 5.2 that we have

$$g^*(\zeta) = (g(\zeta^*))^* = R\left(\frac{\omega(\zeta^*, \alpha)\omega(\zeta^*, \alpha^{-1})}{\omega(\zeta^*, \beta)\omega(\zeta^*, \beta^{-1})}\right)^* = R\left(\frac{\omega^*(\zeta, \alpha)\omega^*(\zeta, \alpha^{-1})}{\omega^*(\zeta, \beta)\omega^*(\zeta, \beta^{-1})}\right) = g(\zeta).$$

Consequently, the fixed equilibria in the circular domain correspond to those in the exterior domain with plates.

6 Conclusion and discussion

We have considered stationary configurations of point vortices in the multiply connected circular domains with the rotational symmetry and the folding symmetry. We first show the invariance of the N-vortex problem in terms of these symmetries. Thanks to this fact, we reduce the system to a one-degree-of-freedom integrable Hamiltonian system, for which the contour plots of the Hamiltonian give us the locations of the fixed equilibria and their stability as saddle and center points. For the circular domains with the rotational symmetry around the origin by the degree $2\pi/M$, all fixed equilibria are the M-rings, in which the point vortices with the identical strength are arranged at the vertices of a regular M-gon. On the other hand, for $N = 2^K$, we have the alternate N-gon in which the point vortices with the positive and negative unit strengths are arranged alternately at the vertices of a N-gon for the circular domains with the K-folding symmetry.

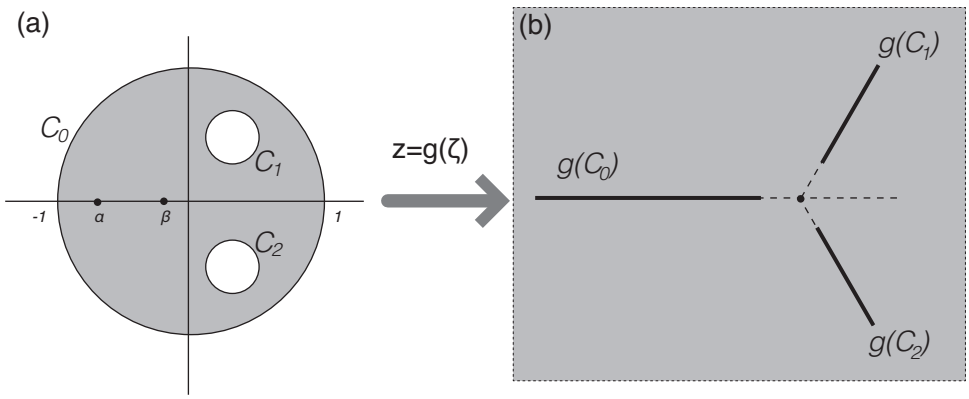

Figure 18: The conformal mapping $z = g(\zeta)$ defined by (31). It maps a circular domain with 1-folding symmetry to an exterior triply connected domain with the same symmetry. Since we have $g^*(\zeta) = g(\zeta)$, fixed equilibria in the circular domain correspond to those in the exterior domain.

We have investigated in depth the bifurcation of the fixed equilibria in the special circular domain $\mathcal{D}_s$ which is invariant with respect to the rotation as well as the folding transformation. There always exists the unstable M-ring near the obstacle and the other two fixed equilibria, one is neutrally stable and the other is unstable, appear due to a saddle-shaped bifurcation. The bifurcation occurs when the ratio between r and a exceeds a certain value that depends on M as long as the obstacles are away from the boundary of the unit circle. We also have identified all fixed equilibria of the four point vortices with the positive and negative unit strengths that has the 2-folding symmetry, which are the alternative rectangles. Then we have discussed their stability and classified the topological patterns of the contour lines of the Hamiltonian. We give a qualitative description of the transition of the topological patterns in terms of the bifurcation of the fixed equilibria and the global reconnection of the separatrices of the contour lines. In both cases, we are unable to find any relative equilibria though the domain acquires the symmetries. This means the M-ring cannot be a relative equilibrium in the circular domain $\mathcal{D}_s$, though it is always a relative equilibrium in the unbounded plane and on the sphere. This fact infers that a few number of relative equilibria of point vortices exist in the multiply connected domains, which should be confirmed in future.

We have discussed fixed equilibria in non circular multiply connected domains. Generally speaking, fixed equilibria in the symmetric circular domains are not always mapped to fixed equilibria in the multiply connected domains with the same symmetries by the conformal mappings. However, if the conformal mappings satisfy the conditions (21) and (23), fixed configuration of the point vortices in the circular domains become those in the multiply connected domains. We give some examples of such conformal mappings that satisfy the sufficient conditions. In particular, the conformal mapping (31) can be applied to the Kasper wing problem to obtain fixed configurations of point vortices that enhance the lift, which will be reported in near future.

Acknowledgements

This study is partially supported by JSPS grants #19654014 and #21340017, and JST PRESTO. I would like to show my gratitude to School of Applied Mathematics at University of Sheffield for providing me with nice research environments during the stay as a visiting scholar.

References

[1] H. Baker, *Abelian functions*, 1995, Cambridge Univ. Press, Cambridge.

[2] D. Bartolucci, *Existence and qualitative properties of concentrating solutions for the sinh-Poisson equation*, IMA J. Appl. Math., 72 (2007), pp. 706–729.

[3] L. J. Campbell and R. M. Ziff, *A catalog of 2-D vortex patterns*, Los Alamos Sci. Report, No. LA-7348-MS.

[4] D. Crowdy and J. Marshall, *Analytical formulae for the Kirchhoff-Routh path function in multiply connected domains*, Proc. Roy. Soc. A, 461 (2005), pp.2477–2501.

[5] D. Crowdy and J. Marshall, *The motion of a point vortex around multiple circular islands*, Phys. Fluids, 17 (2005) 056602.

[6] D. Crowdy, *The Schwarz-Christoffel mapping to bounded multiply connected polygonal domains*, Proc. Roy. Soc. A, 461 (2005), pp.2653–2678.

[7] D. Crowdy, *Analytical solutions for uniform potential flow past multiple cylinders*, Euro. J. Mechanics B/Fluids, 25 (2006), pp.459–470.

[8] D. Crowdy, *Calculating the lift on a finite stack of cylindrical aerofoils*, Proc. Roy. Soc. A, 462 (2006), pp.1387–1407.

[9] D. Crowdy and J. Marshall, *Conformal mappings between canonical multiply connected domains*, Comp. Methods Funct. Theory, 6 (2006), pp.59–76.

[10] M. Flucher and B. Gustafsson, *Vortex motion in two dimensional hydrodynamics*, TRIATA-MAT-1997-MA 02, Stockholm, Royal Institute of Technology.

[11] D. Lewis and T. Ratiu, *Rotating n-gon/kn-gon vortex configurations*, J. Nonlinear Sci., 6 (1996), pp. 385–414.

[12] C. C. Lin, *On the motion of vortices in two dimensions. II. Some further investigations on the Kirchhoff-Routh function*, Proc. Natl Acad. Sci., 27, (1941) pp. 575–577.

[13] C. C. Lim, J. Montaldi and M.R. Roberts, *Relative equilibria of point vortices on sphere*, Physica D, 148 (2001), pp. 97–135.

[14] F. Laurent-Polz, *Point vortices on the sphere: A case of opposite vortices*, Nonlinearity, 15 (2002), pp. 143–171.

[15] Z. Nehari, *Conformal mapping*, New York, McGraw-Hill (1952).

[16] P. K. Newton, *The N-vortex problem, Analytical techniques*, Springer-Verlag, New York, 2001.

[17] P. G. Saffman and J. S. Sheffield, *Flow over a wing with an attached free vortex*, Stud. Appl. Math., 57 (1977), pp. 107–117.

[18] T. Sakajo, *Explicit representation of point-vortex interaction in multiply connected circular domains*, Proc. Roy. Soc. A, 465 (2009), pp. 2589–2611.